2018

# ANALYSIS OF UNDERGROUND COAL MINE STRUCTURES SUBJECTED TO DYNAMIC EVENTS

Brooklynn Yonts
*University of Kentucky*, brooklynn_yonts@outlook.com
Digital Object Identifier: https://doi.org/10.13023/etd.2018.446

STUDENT AGREEMENT:

I represent that my thesis or dissertation and abstract are my original work. Proper attribution has been given to all outside sources. I understand that I am solely responsible for obtaining any needed copyright permissions. I have obtained needed written permission statement(s) from the owner(s) of each third-party copyrighted matter to be included in my work, allowing electronic distribution (if such use is not permitted by the fair use doctrine) which will be submitted to UKnowledge as Additional File.

I hereby grant to The University of Kentucky and its agents the irrevocable, non-exclusive, and royalty-free license to archive and make accessible my work in whole or in part in all forms of media, now or hereafter known. I agree that the document mentioned above may be made available immediately for worldwide access unless an embargo applies.

I retain all other ownership rights to the copyright of my work. I also retain the right to use in future works (such as articles or books) all or part of my work. I understand that I am free to register the copyright to my work.

REVIEW, APPROVAL AND ACCEPTANCE

The document mentioned above has been reviewed and accepted by the student's advisor, on behalf of the advisory committee, and by the Director of Graduate Studies (DGS), on behalf of the program; we verify that this is the final, approved version of the student's thesis including all changes required by the advisory committee. The undersigned agree to abide by the statements above.

Brooklynn Yonts, Student

Dr. Jhon Silva, Major Professor

Dr. Zacharias Agioutantis, Director of Graduate Studies

# ANALYSIS OF UNDERGROUND COAL MINE STRUCTURES SUBJECTED TO DYNAMIC EVENTS

---

THESIS

---

A thesis submitted in partial fulfillment of the requirements for the degree of Master of Science in Mining Engineering in the College of Engineering at the University of Kentucky

By

Brooklynn Yonts

Lexington, Kentucky

Director: Dr. Jhon Silva , Professor of Mining Engineering

Lexington, Kentucky

2018

ABSTRACT OF THESIS

# ANALYSIS OF UNDERGROUND COAL MINE STRUCTURES SUBJECTED TO DYNAMIC EVENTS

Underground coal mine explosions pose a significant threat to infrastructure such as mine seals and refuge alternative chambers. After a mine seal failed in the Sago mine disaster, which took the life of 12 miners, design requirements were reexamined and improved. However, most research being completed on the analysis of mine structures during an explosive event focuses solely on peak pressure values, while ignoring the impact of pressure duration. This study investigates the impact pressure duration, waveform shape, and impulse have on structural displacement, while also exploring what pressures and durations can be expected during a mine explosion. Additionally, the use of high explosives to simulation conditions experienced during a mine explosion is examined. Results from this study are produced through experimental testing using a scaled shock tube and theoretical studies using finite element analysis.

KEYWORDS: Impulse, Finite Element Analysis, Pressure Profiles, Structural Analysis, SDOF System

Brooklynn Yonts

*12/05/2018*

# ANALYSIS OF UNDERGROUND COAL MINE STRUCTURES SUBJECTED TO DYNAMIC EVENTS

By

Brooklynn Yonts

Dr. Jhon Silva
Director of Thesis

Dr. Zacharias Agioutantis
Director of Graduate Studies

*12/05/2018*

# Dedication

I would like to dedicate this thesis to the old man who told me to leave, because women are bad luck in mines.

# Acknowledgements

The research completed in this thesis was made possible thanks to multiple individuals and groups. First, I would to thank members of the University of Kentucky Explosives Research Team for enduring both heat waves and snow showers while collecting data for my research. Also I would like to thank the Nally and Gibson Georgetown operation, for allowing us to conduct research testing on their mine site. Additionally, there many professors within the mining department that have motivated me to pursue my graduate degree, I would like to specifically thank Dr. John Groppo for his guidance in preparing coal dust for testing and for allowing access to the processing laboratory. I would also like to thank my advisor Dr. Jhon Silva. The world of academia is often considered cold and pragmatic. During my time as both a teaching and research assistant under Dr. Silva, I have learned he is creative, patient, and kind. He has given me the chance to take part in meaningful research while also challenging me to grow as an individual. I would also like to thank Dr. John Groppo and Dr. Zacharias Agioutantis for serving on my graduate committee. Lastly, I would like to acknowledge the National Institute for Occupational Safety and Health. Without research projects, funded by NIOSH, this study would not have been possible.

# Table of Contents

# List of Tables

# List of Figures

# 1 Chapter 1: INTRODUCTION

## 1.1 Introduction/Background:

This chapter provides an introduction to the topics studied in this thesis along with their significance. Three research questions are introduced, that serve as the framework for the entire thesis and its results. Key terms and procedures are also included here.

While many mining methods rely on controlled explosions to break rock for excavation, underground coal mining operations go to great lengths to prevent them from occurring. Even controlled blasting in underground coal mining has become an obsolete technique with the introduction of the continuous and longwall mining methods. In general, unwanted explosions can result from a variety of sources. In underground coal mines, the most anticipated source of an explosion comes from combining the ignition of methane gas in the presence of coal dust. This deadly combination has led to catastrophic events like the Upper Big Branch disaster, which killed 29 miners in 2010.

United States underground coal mining regulations focus on mitigating the threat of explosions by requiring the use of rock dust, ventilation controls, and gas monitoring. However, because the hazard of a coal mine explosion cannot be eliminated, engineers must design underground structures to withstand the extreme conditions experienced during an explosive event. Specifically, the design of explosion resistant mine seals has been a focus of research in recent years.

Seals are structures built to separate unused or already-mined areas from active areas of underground mines. Even with the high monetary cost of constructing a seal, they ultimately save operations time and money by reducing the ventilation load and the area to be monitored. After an explosion in a sealed area of the Sago mine in West Virginia, which lead to the death of 12 miners, the National Institute for Occupational Safety and Health (NIOSH) completed research projects to ultimately recommended the following flowchart for seal design. As shown in Figure 1, the design recommendations of 50, 120, and 640 psi are based on mine characteristics such as monitoring and run-up length (Zipf, Brune, & Thimons, 2009). All peak pressures recommendation in Figure 1 are larger than the 20 psi requirement that was in place for seal design during the Sago disaster.

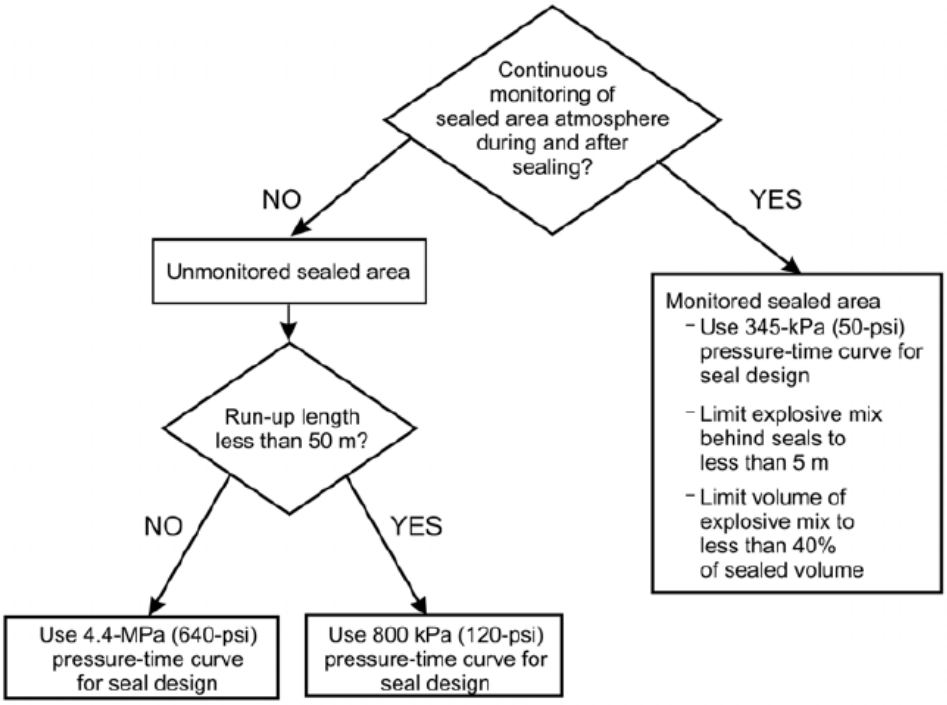


*Figure 1: NIOSH Seal Design Selection (Zipf, Brune, & Thimons, 2009).*

Currently, common engineering practices involve seals designed to withstand specific peak pressures experienced during a mine explosion, while ignoring the structural effects of rise time duration and pressure decay. This research, through experimental testing and numerical analysis, examines characteristic waveforms produced by methane gas, and their implications in the structural response of underground coal mine structures, such a mine seals.

## 1.2 Statement of the Problem

There are clear peak pressure design requirements for underground coal mine structures, such as seals and refuge chambers. However, there is limited evidence demonstrating the effects of pressure duration on structural response.

## 1.3 Conceptual Framework for the Study

The energy of an explosive event can be thought of as the integral of the pressure-time curve recorded during an explosion. This energy is referred to as the impulse. Different types of explosions will produce different pressure profile shapes. High explosives tend to have shorter durations but higher peak pressure values. Low explosives tend to have longer durations but with lower peak pressure values.

Underground coal mine explosions are unique in that they combine both dust and gas explosions into one event. Generally, this blend of explosive properties creates a pressure profile shape close to that of a low explosive. While peak pressure values can be a useful way to describe the intensity of an explosive event, the duration of pressure can also affect the structural responses.

## 1.4 Purpose of Study and Research Questions

This thesis aims to improve the understanding of underground coal mine explosions and provide aid to studying them in a laboratory setting. The study intends to provide information that can contribute to design recommendations for underground structures in the future. While much of the mining legislation in place today was created in response to specific mine disasters, knowledge held today can potentially prevent further deaths in the mining industry and should be investigated now, not after another explosion has occurred.

Ultimately, three questions are investigated in this research:

1. What types of peak pressure values and pressure duration can be expected during a coal mine explosion?
2. How does the impulse of an explosion effect the displacement of simple structures?
3. Can high explosives, such as C4, be used to simulate coal dust and methane explosions?

It is hypothesized that methane coal dust explosions will more closely correspond to a low order explosion. However, the increase in pressure duration could also lead to an increase in the impulse that would influence structural displacement to a larger degree. Lastly, if the impulse of an explosion using high order explosives equals that of low order explosives, the resulting displacements will be similar.

## 1.5 Procedures

Pressure profiles for analysis were collected using a scaled shock tube operated by the University of Kentucky Explosives Research Team (UKERT). Data acquisition systems, including piezoelectric sensors, were used to record dynamic pressure readings during both high and low order explosive events. Methane was used to model a low order explosive event, and a detonator containing PETN was used to model a high order explosive event.

A single degree of freedom system (SDOFS) in one dimension and three dimension was used to analyze structures under pressure loading during an explosive event. This was done with hand calculations and with a finite element analysis (FEA) software (MSC Patran/Natran/Dytran).

Comparisons between structural displacements based on impulse values were made to compare the impact of pressure duration and peak pressure values on structural designs.

## 1.6 Significance of the Study

Even with declines in the United States' coal market, 253 underground coal mines were still operational in 2016 (EIA, 2017). If an underground explosion like Sago, Darby, or Upper Big Branch were to occur again, the women and men working in these active mines could be put at an even greater risk if underground structures such as seals and refuge chambers fail. The United States government responded to the Sago crisis by requiring an increased strength of seal design. Instead of continuously acting in response to catastrophic events, engineers should be obligated to improve safety through research before designs are tested in real world events.

This study provides information to assist in that type of preventative research in multiple ways. Understanding the characteristics of a methane and coal dust explosion leads to a greater comprehension of the impulses created. Knowing what level of impulses can be expected from a mine explosion allows for the analysis of the structural response that could occur from them. Providing information about these topics, and how to continuously enhance our ability to study mine explosions in a laboratory setting will help engineers better prepare for the next potential mine explosion, which ultimately can reduce the number of lives lost during a disaster event.

## 1.7 Limitations of the Study

This evaluation was done assuming that materials remain in the elastic region of the stress-strain curve. Further material properties could be introduced to the SDOF system to represent the response materials have to strain rate.

Additionally, tests for this research were complete in a small scale shock tube. Further test should be completed in a large scale shock tube to more closely resemble real mine conditions.

The results of this study are meant to highlight the impact pressure duration has on impulse and ultimately structural displacement. Changes in design requirements and guidelines are not recommended as a result of this research, but rather should be analyzed with this consideration in mind.

## 1.8 Organization of the Study

The chapters of this project are outlined in the Table of Contents section. They cover a literature review and provide pertinent background information before describing data

collection and data analysis. Results are presented along with concluding remarks and recommendations for future works. Relevant data is presented within the body of the thesis, with additional data and information included in the attached appendices.

## 1.9 Definition of Terms

| | |
|---|---|
| $t_a$ | Arrival time of shockwave at some distance from the source |
| $p_0$ | Ambient pressure |
| $P_s^+$ | Peak positive overpressure during the explosion |
| $P_s^-$ | Peak negative pressure during the explosion |
| $T^+$ | Time of positive phase of the ideal pressure curve |
| $T^-$ | Time of negative phase of the ideal pressure curve |
| $\mathrm{I}^+$ | Positive Impulse |
| $\mathrm{I}^-$ | Negative Impulse |
| $W$ | Weight |
| $k$ | Spring constant |
| $g$ | Force of gravity |
| $T$ | Natural Period |
| $k$ | Ratio of force to deflection of the beam |
| $c$ | Damping constant |

# 2 Chapter 2: LITERATURE REVIEW

This chapter serves as a comprehensive review of previous work completed in the areas of coal mine explosions and explosion research testing.

Coal mines are inherently at risk for explosions because both methane gas and coal dust are produced during the mining method (du Plessis, Saleh, & Phillips 2017). If an ignition source comes in contact with a pocket of methane, there is a rapid expansion of methane/air mixture that creates a shockwave. This shockwave displaces and disperses coal dust which is then ignited by the flame produced during the initial methane explosion. This disturbance disperses additional coal dust and creates a self-sustaining process (du Plessis, Saleh, & Phillips 2017).

Understanding how coal mine explosions occur and propagate is the first crucial step in designing structures to withstand them. This literature review outlines previous work completed on the subject of coal mine explosions, corresponding to each of the three research questions provided in Chapter one.

## 2.1 Peak pressure values and pressure durations expected during a coal mine explosion

In 1985, the US Bureau of Mines designed a 20-L chamber for testing dust and gas explosions. At that time, the popular "Siwek" 20-L chamber was also widely used, with both options providing comparable results (Cashdollar & Hertzberg, 1985). Over the past 30 years, considerable research has been completed using 20-L chambers virtually identical to these original designs (Eades, Perry, Johnson, & Millar, 2018). Under controlled conditions, these chambers allow researchers to carefully measure and record important explosion characteristics such as: explosion pressures, rates of pressure rise, minimum ignition energies, and minimum/maximum gas concentrations (Cashdollar & Hertzberg, 1985).

Kenneth Cashdollar, both pioneer and expert in the field of dust explosions, has numerous publications based on research using 20-L chambers. In his 1996 work, Cashdollar recorded the explosion pressures from coal-air explosions and methane-air explosion independently. His work has helped quantify pressure values expected from various concentrations of dust and gas. Shown in Figure 2, the peak pressure values for a methane-air explosion were approximated at 120psi and 95psi for coal dust (Cashdollar, 1996).

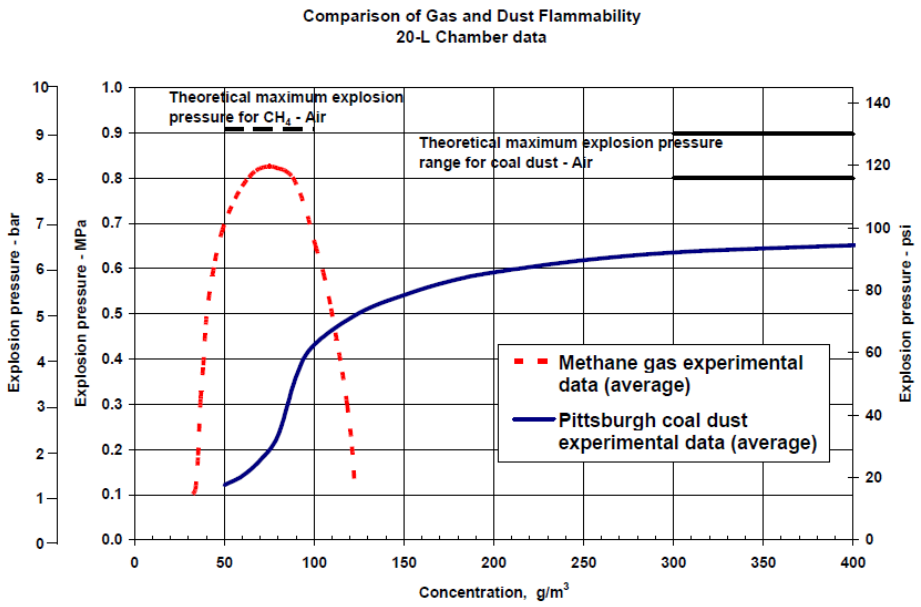


*Figure 2: Graph of Variations of Absolute Pressure for Methane-air and Coal Dust-air Explosions (Cashdollar 1996)*

Generally, mine explosions are considered hybrid explosions that have characteristics resulting from a mix of both methane and coal dust igniting. Ajrash, Zanganeh, and Moghtaderi (2016) ignited hybrid coal gas mixtures in a 20-L chamber and recorded peak pressures of approximately 87 psi when concentrations of 50 g/m$^3$ dust were mixed with 5% methane gas.

Chamber testing can be used to study explosion parameters and has become an industry standard. However, results found in small-scale testing chambers do not always transfer successfully to describe full-scale events (Chawla, Amyotte, & Pegg, 1996). Representing realistic turbulent flows and deposition scheme can be difficult while also trying to avoid under and over driving (Eades et al., 2018). Over-driving occurs when the dust cloud ignition source burns the dust and preheats the cloud, this intensifies the severity and potential for an explosion. In contrast, under-driving occurs when chamber walls cool the flame front and lower the severity and potential for an explosion. Additionally, in both longwall and room-and-pillar operations, the potential areas of explosive gases can be extensive, as in gob areas and behind seals. For this reason, large-scale testing facilities like the Lake Lynn Experimental Mine (LLEM), have played an important role in studying mine explosions.

The former limestone mine (LLEM), located in Fairchance Pennsylvania (Sapko et al., 2000), conducted coal mine explosion testing in full-size drifts. As described by Sapko, Weiss, Cashdollar, and Zlochower (2000), plastic diaphragms were used to section off 15 m pockets of methane gas. Electric matches were used to ignite gas mixtures. The resulting pressure waves propagated down entries where coal dust was dispersed on both shelves

and the floor. In testing using both methane gas and a dust concentration of 200 $g/m^3$, maximum pressures were recorded at approximately 6 bar (87 psi) (Sapko et al., 2000). While not the focus of their study, graphs provided in (Sapko et al., 2000) show pressure durations of 50-100ms. As of 2013 however, the LLEM was closed and no longer conducts testing.

Another source providing insight to expected blast pressures comes from MSHA accident reports. In their research, QinetiQ North America and Foster-Miller Inc (2008) reviewed 32 MSHA reports of mine accidents. From those reports, 19 involved explosions and 6 provided estimates of blast pressures. From this information, the estimated peak pressure values for methane only explosions range from 4 to 22 psi. With the addition of coal dust, those values were shifted to 12-20 psi. This report also estimated 45 psi as the pressure of an ideal methane-air explosion.

Just months after the completion of Foster-Miller's report, a massive explosion occurred in Montcoal, West Virginia at the Upper Big Branch (UBB) mine. With maximum pressures more than twice those reported by Foster-Miller, UBB experienced estimated reflective pressures of 105 psi (Hedrick & Nicola, 2011). Reflective pressures can be 2 to 8 times greater than the incident overpressure and arise from a change in momentum when moving air strikes a surface and changes direction (Glasstone & Dolan, 1977).

In addition to the consideration of reflective pressures, Nagy (1981) describes the two types of pressures created during a coal mine explosion as dynamic and static. Static pressure is created from expanding combustions products and is equal in all directions. Static pressure is measured in closed volumes. Dynamic pressure results from air propagating through a mine. The flow of gases at high speeds creates dynamic pressure in one direction (Nagy, 1981). In chamber testing, static pressures have been measured at 101 psi (Sapko et al., 2000). In the Bruceton experimental mine, pressures of 10 bar (145 psi) have been developed (Nagy, 1981). This higher pressure value could result from pressure piling, a phenomenon that happens when fuel-rich air ahead of the explosive front is compressed and then burns at an increased pressure (Sapko et al., 2000). If an explosion transitions from deflagration to detonation, the explosion pressures may double (Kuchta, 1985).

In summary, there are various methods for studying coal dust and methane explosions. Small-scale lab test may not always provide comparable results to full-scale events. Conducting full-scale test is difficult and expensive. For this reason, there are very few facilities where this testing can take place. With infinite mine layouts possible, the influence of reflected pressures, deflagration to detonation transitions, and pressure piling, peak pressures to be expected from a mine explosion are difficult to predict. Still, most studies focus primarily on the peak pressures experienced during a blast event, with little emphasis on pressure duration.

## 2.2 How impulse effects the displacement of simple structures

Baker (1973) provides a detailed description of the rapidly expanding chemical process that occurs during an explosion as shockwaves are created. The rate of this expansion is used to classify explosives. Coal dust and methane are considered low explosives. Also known as combustion explosives, these materials decompose through deflagration and produce shockwaves that move slower than the speed of sound (3000 fps). In contrast, high explosives detonate and have shockwaves that move faster than the speed of sound. (Agrawal & Bhattacharya, 2014)

Shockwaves deliver overpressures, or pressures above normal atmospheric pressure, to surrounding areas. This pressure, recorded over the duration of the explosive event, is referred to as a pressure profile. Pressure profiles are an effective tool for describing and comparing explosive events, with the two most crucial parameters being the peak pressure and impulse (Alonso et al., 2006).

Baker (1973) describes an ideal pressure profile, as one occurring in a still, homogenous atmosphere. His report provides the ideal pressure-time curve in Figure 3. Here, an instantaneous peak pressure ($P_0$-$P_s^+$) is experienced at the arrival time $t_a$, then quickly decays to a small peak negative pressure ($P_0$-$P_s^-$). The ideal pressure curve is divided into two phases: positive and negative.

Using the definitions provided by Baker (1973), the impulse of an explosion can be defined as the integral of the $p(t)$ function. As given below, $I^+$ and $I^-$ correspond to the positive and negative impulses respectively.

$$I^+ = \int_{t^a}^{t^a+T^+} (p(t) - p_0)dt \qquad [1]$$

$$I^- = \int_{t^a+T^+}^{t_a+T^++T^-} \big(p_0 - p(t)\big)dt$$

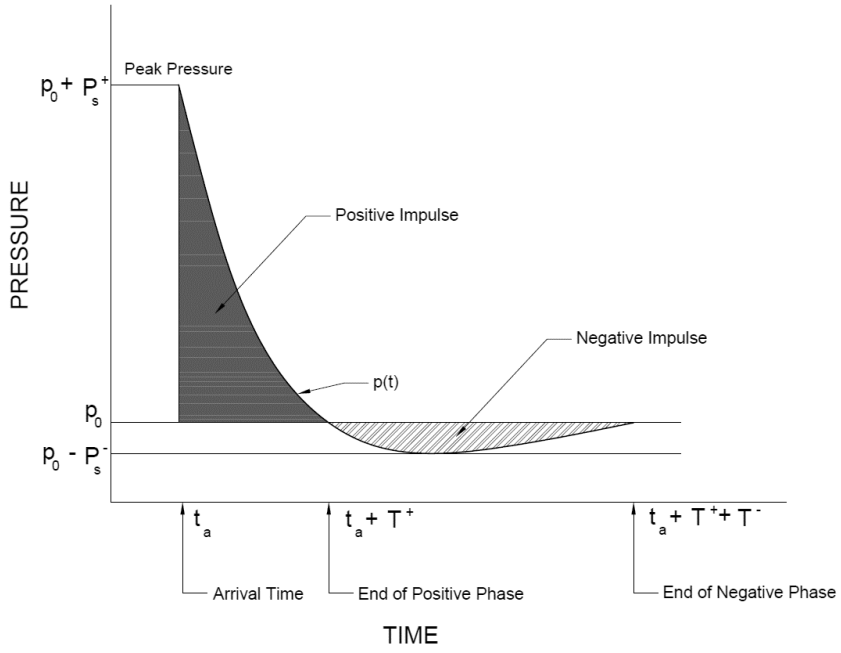


*Figure 3:Ideal Blast Wave Pressure-Time Curve*

To directly illustrate the impact wave shape, and ultimately impulse, has on physical structures, a numerical analysis of one-dimensional system can be implemented. Biggs (1964) provides an outline for approximating deflection with a single degree of freedom (SDOF) structures. Using a concentrated mass and weightless spring to represent an equivalent real structure, a direct analysis applying partial differential equations and finite differences can be completed to determine the deflection of the system in one direction during dynamic loading. Ngo, Mendis, Gupta, and Ramsay (2007) introduce this SDOF method as a foundation for studying deflections before introducing CFD (computational fluid dynamics) as a method to predict structural responses. Both methodologies are implemented and presented in this thesis. Ngo et al. (2007) also explain that because blast-induced pressure fields on structures are of highly nonlinear behavior, predictive modeling must be validated through experimental testing, which was also a priority when completing this thesis.

As provided by Biggs (1964), the natural period of a one-degree system is given by the following equation:

$$T = 2\pi \sqrt{\frac{W}{kg}}$$

*[2]*

The relationship between a structure's natural period and the duration of the positive pressure phase during a blast event also plays a crucial part in predicting displacement. As shown in Figure 4, Karlos and Solomos (2013) present this relationship using a Pressure-Impulse Diagram. As the ratio of pressure duration to natural period increases, the type of loading a structure experiences moves from impulsive to dynamic, and then to quasi-static. For short pressure durations, less than one-fourth of the natural period, structures become more sensitive to impulse values than peak pressure values. As the load duration increases, structural response becomes more sensitive to peak pressure values (Karlos & Solomos 2013).

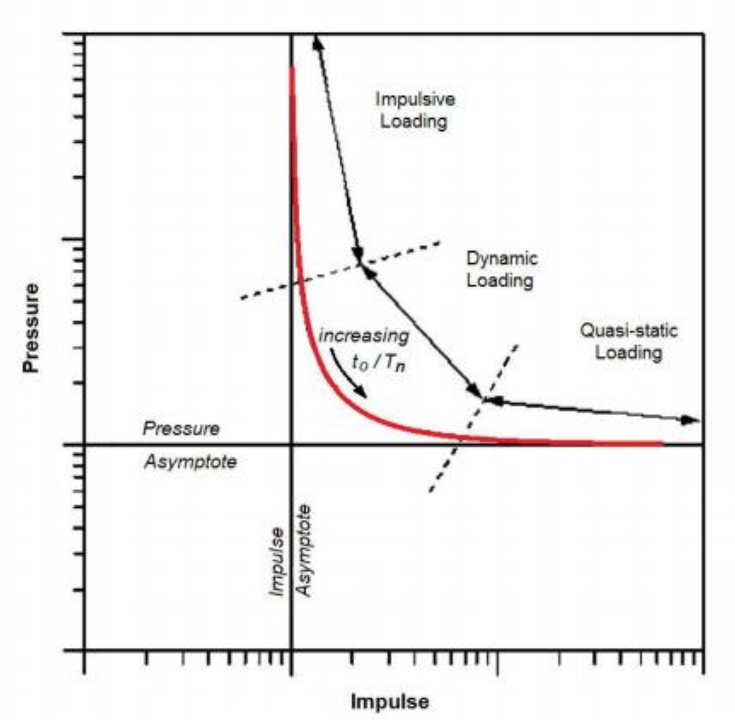


*Figure 4: Pressure-Impulse Diagram (From Karlos and Solomos 2013)*

Figures 5-7 show three recommended design curves provided by NIOSH for seals built in underground coal mines within the United States. The selection of a design curve is based on the criteria given in Figure 1. The main distinction between curves comes from their peak pressure values of 50, 120, and 650 psi (Zipf et al., 2009). However, the duration of each design curve is extended to a time of 1 second. This arbitrary selection of duration length greatly affects the impulse for each profile and ultimately would affect displacement as well.

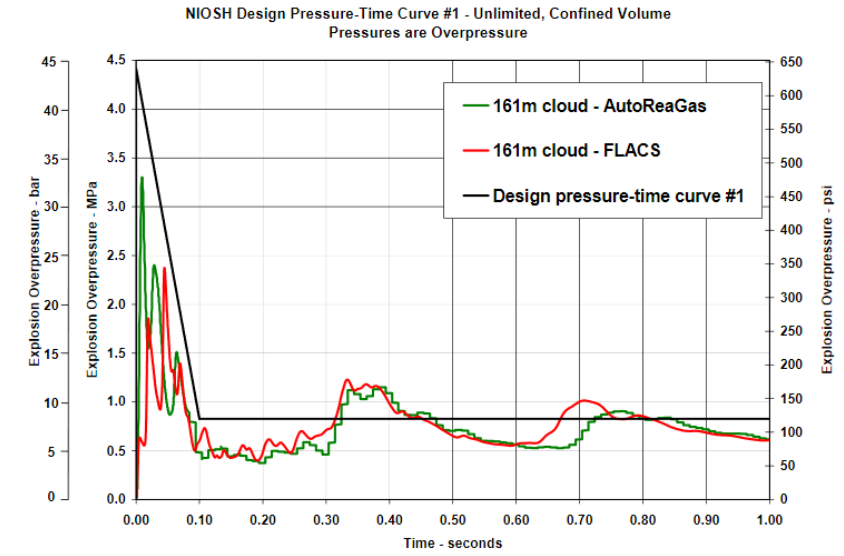


*Figure 5: NIOSH Design Curve 1 (Zipf et al. 2007)*

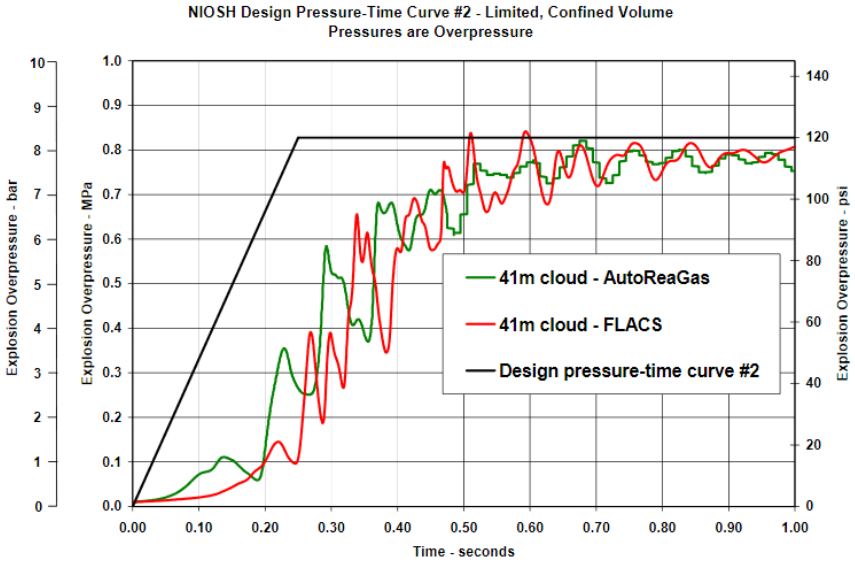


*Figure 6: NIOSH Design Curve 2 (Zipf et al. 2007)*

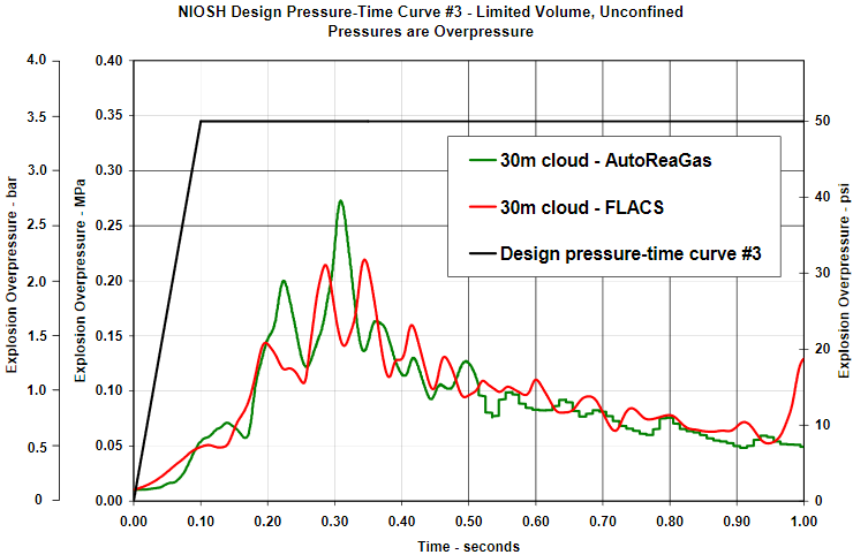


*Figure 7: NIOSH Design Curve 3 (Zipf et al. 2007)*

It should be noted that since the introduction of explosion-resistant seals, after the Sago Mine explosion, MSHA has conducted detailed evaluations of all proposed seal designs. Such test includes work completed by Sapko, Harteis, and Weiss (2008). In their work, the U.S. Army's Wall Analysis Code (WAC), a SDOF model developed to study walls subjected to blast loads, was used to calculate seal deflection using simulated pressure histories. Figure 8 and Figure 9 show the five pressure profiles used in testing and their resulting displacements. Here, each profile has a different rise time. The resulting displacements vary significantly based on this rise time. Sapko et at. (2008) point out that after the rise time becomes greater than the natural frequency of the seal (8ms), the displacements become smaller.

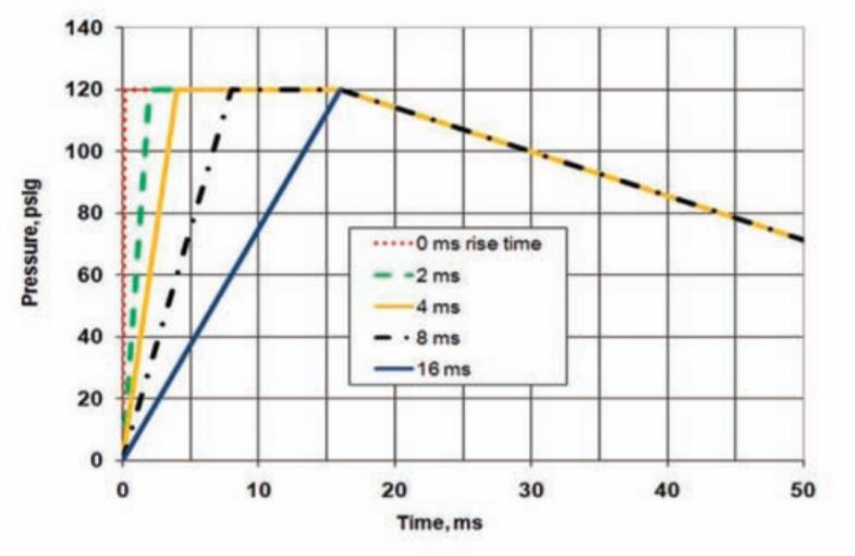


*Figure 8: Simulated pressure histories (Sapko et al. 2008)*

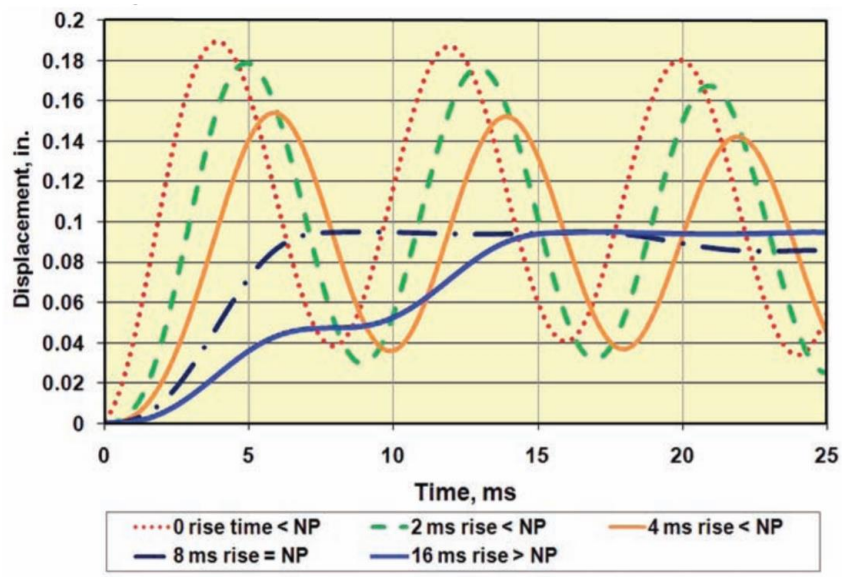


*Figure 9: Seal Displacement (Sapko et al. 2008,*

In the Sapko et at. (2008) paper, no indication of pressure duration is provided, nor is the impulse for each pressure profile discussed.

## 2.3 Using high explosives to simulate coal dust and methane explosions.

If possible, experimental research developed to better understand coal mine explosions should represent realistic conditions as closely as possible. As previously stated, the Lake Lynn Experimental Mine could conduct blast research is a representative and controlled location. The facility, that conducted research from 1982-2011, was rare. Today, there are very few testing facilities around the world that can conduct full-scale mine explosion

testing. Such facilities include the Kloppersbos facility in South Africa (Humphreys, Collecutt, & Proud 2010) and the SIMTARS facility in Australia (Wu, Gillies, Oberholzer, & Davis 2009).

The construction of new full-scale testing facilities is costly and often not a practical option. Additionally, because coal methane explosions are a naturally occurring phenomenon, they can be difficult to control and introduce issues in both repeatability and safety. For these reasons, commercially made high explosives are sometimes used to replicate an underground mine explosion in experimental research. Composition C-4 has been used to model a mine explosion for rock dust testing (Eades, 2016). As well as in the development of polycarbonate walls used in underground coal mines (Meyr, 2013). In his thesis, Rex Meyr references the concern of using high explosives to mimic coal mine explosions, in that the waveform shape of the time-pressure curve for a high explosive (C-4) is different from that of a low explosive (coal dust).

This thesis looks at the possibility of using multiple delayed blast of high explosives to mimic the pressure profile of a low explosive. This methodology would allow for researchers to carefully monitor and regulate expected peak pressure values and have impulse values more closely resembling those found in underground mine explosions.

# 3 Chapter 3: EXPERIMENTAL SETUP

Chapter three outlines the experimental setups used to complete testing for this thesis. This includes testing with methane, coal dust, and high explosives. Additional information about the coal dust used for testing is included in this chapter along with the specific equipment used to collect data. Heat interference for pressure transducers is introduced and discussed.

## 3.1 Pressure Profile Recording

It was desired that both the SDOF and FEA analyses implement realistic pressure profiles, representative of those found in coal mine explosions. To accomplish this, experimental testing was completed to record pressure profiles for methane and PETN explosions. The test took place in a 19-foot scaled shock tube, constructed from steel, with a square cross-sectional area of one squarefoot. The shock tube served as a means to contain the explosion, while also directing the created pressures along its length. The individual testing procedures are as follows.

### *3.1.1 Methane Testing Procedure*

Figure 10 shows the various components used to create a controlled methane explosion. The attached driver section of the shock tube (painted white) houses a simple fan blade that can be turned using an impact wrench attached to the fan axle. The fan blade mixes methane that is added to the bottom of a chamber via a gas line, where a ball valve is used to control the inflow of methane to the tube. Two infrared methane gas detectors record methane concentrations from 0 to 100%, using pumps and specially designed tubing. The gas detectors used are iBird MX6 devices, which have an accuracy of ±5.0%. Plastic membranes, approximately 2mm thick, are used to contain the methane/air mixture until ignition. The concentrations were monitored and ignited at approximately 10% methane. Electric matches, placed 6 inches from the top of the tube, were chosen as an ignition source because their ignition does not add external pressure to the explosive event.

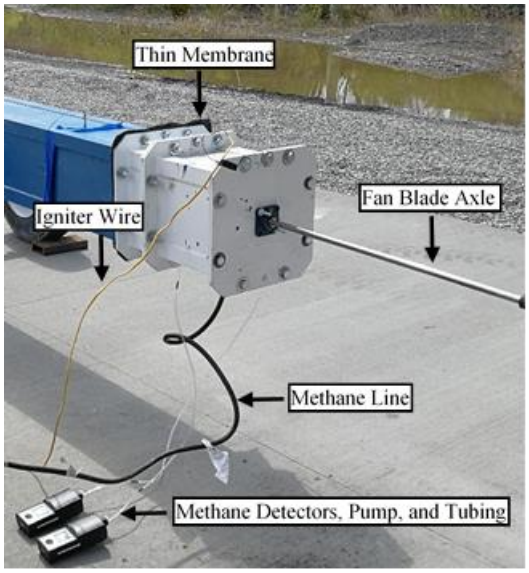


*Figure 10: Methane Testing Setup*

### *3.1.2 Detonator Testing Procedure*

A commercial detonator (electric blasting cap), containing the high explosive PETN, was used to create a high order explosion. The blasting cap was located 6 inches from the top of the driver section and connected to the ignition wire. The cap was initiated using a blasting machine. Because no explosive air mixture was used in this test, no methane, membrane, gas monitoring, or fan were used in this testing setup.

### *3.1.3 Data Collection*

It was determined that pressure recordings for both methane and PETN explosions would be taken from the same pressure sensor location, which was located approximately 8 feet from the ignition location. Methane and PETN test were completed independently and multiple times. PCB Piezoelectric pressure sensors, with peak measuring pressures of 50psi, thread into the wall of the shock tube until the diaphragm of the sensor is flush with the interior wall. The pressure sensors are connected to a signal conditioner that provides power to the sensors and transfers the recorded signals to a DataTrap device. The DataTrap is programmed to record pressure readings when an appropriate explosion pressure is experienced. Recordings are then transferred from the DataTrap to a computer, where they can be analyzed using the graphing software Dplot. A general representation of the Data Acquisition components is given in Figure 11. The results recorded during the testing described here can be found in Chapter four.

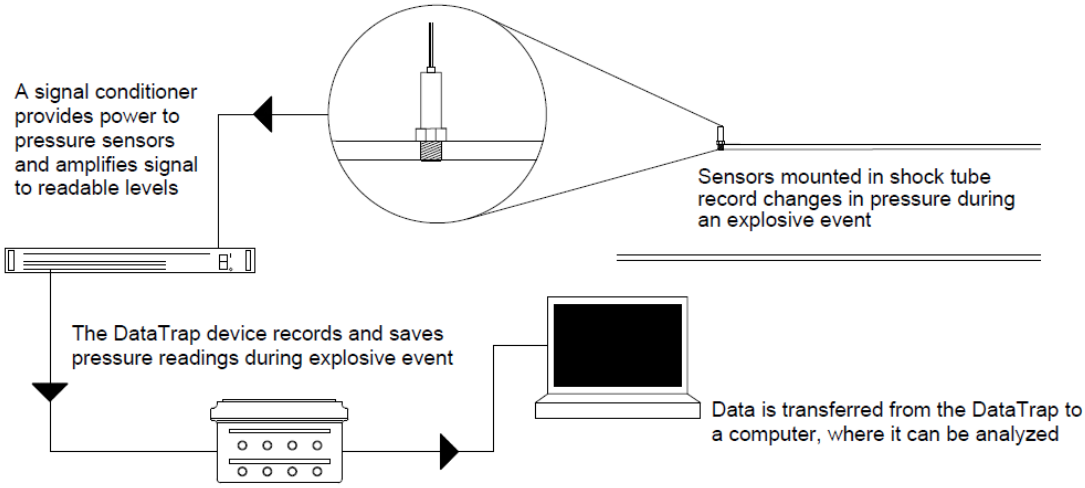


*Figure 11: Data Acquisition Setup*

### *3.1.4 Coal Dust Preparation and Dispersion*

The procedure followed to create coal dust, used in future testing, is described here. Throughout the mining process, coal dust is inherently created. It can accumulate under beltlines and on equipment. However, coal dust must be artificially created for laboratory test. The desired size distribution for dust used in testing for this thesis was modeled after samples used by NIOSH for various explosion prevention testing. Figure 12 shows a plot of the cumulative size distributions for both the NIOSH dust sample and the sample created.

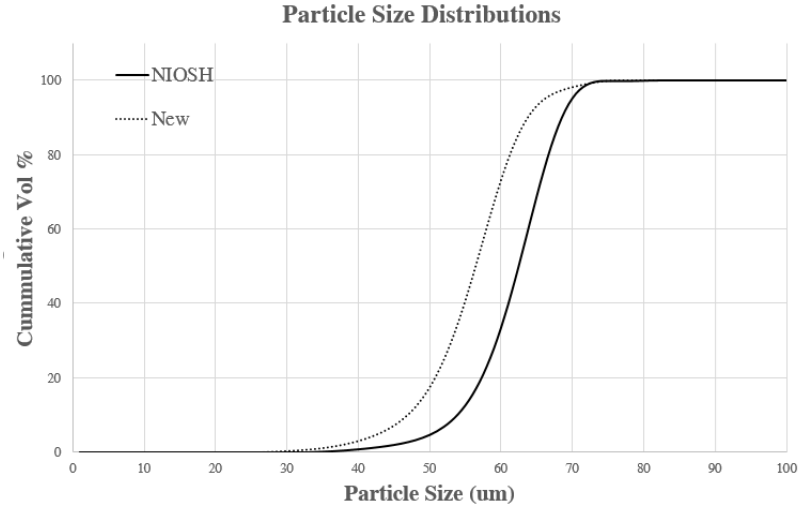


*Figure 12: Coal Dust Size Distributions*

The dust used for testing was created from coal collected at the Hamilton County coal mine in Dahlgren, Illinois. Raw coal was processed using a laboratory jaw crusher in conjunction

with two hammer mills, each decreasing in throughput size. To achieve a fine dust, the sample was also placed in a wet ball mill and ground for 2.5 minutes. A proximate analysis was also completed for the sample, with the results listed in Table 1.

*Table 1: Coal Qualities*

| | |
|---|---|
| Moisture | 5.35% |
| Dry Ash | 16.98% |
| Dry Volatile | 36.44% |
| Dry Fixed Carbon | 46.58% |

For testing including coal dust, the following procedure was followed to disperse the dust within the shock tube prior to ignition. A 2x4 measuring 10 feet was used to load coal from each end of the shock tube. The wood was marked at one-foot intervals to aid in the even dispersion of dust along the length of the beam. Dust was weighed and distributed evenly before the beam was loaded into the shock tube and flipped to disperse the coal dust onto the bottom of the tube. Various dust concentrations were tested, with a concentration of $150 g/m^3$ being optimal.

## 3.2 Recording Coal Dust and Methane Explosions

As previously described, it is the combination of a fuel air mix igniting a self-propagating suspended dust cloud that makes coal mine explosions distinctively hazardous. For this reason, it was desired that explosions containing both methane and coal dust would be studied for this thesis. While high explosives do produce elevated temperature during their detonation, methane and specifically the burning of coal dust creates hotter temperatures for longer periods of time. This increase in temperature during testing produces difficulties in recording correct pressure values using piezoelectric sensors.

As the prefix piezo indicates, piezoelectric sensors contain material that generates a voltage when deformed of squeezed. Piezoelectric sensors are often used for pressure monitoring in blast testing because of their ability to measure dynamic events and their durability. However, when piezoelectric sensors are exposed to very high temperatures the detection material can expand and this expansion can cause inaccurate pressure recordings as shown in Figure 13.

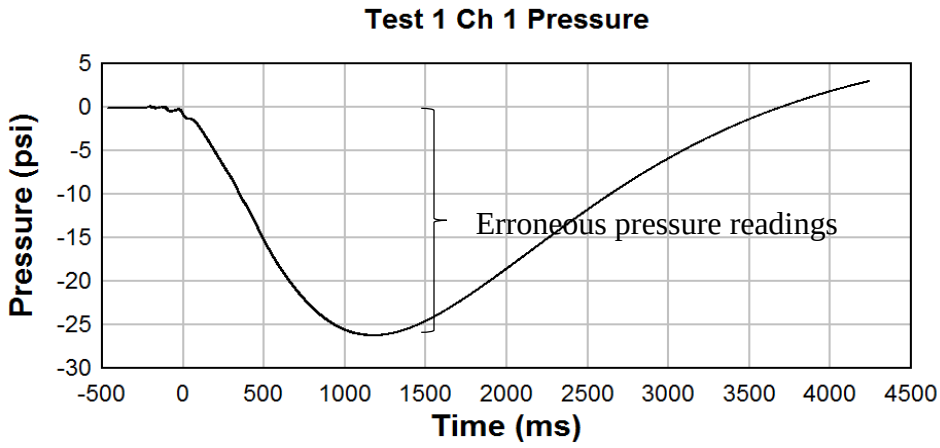


*Figure 13: Heat Effect on Pressure Readings*

Over the past year, the UKERT team has researched multiple approaches to recording pressure values in high temperature events, such as methane and coal dust explosions, and has made significant improvements in the experimental testing setup. Details of this research are included here.

### *3.2.1 Temperatures Experienced During Testing*

Before potential solutions could be tested, it was important to discern what range of temperatures testing equipment would be exposed to and must withstand during testing. To answer this question, a CMH1 Optris temperature probe was used. The probe has a response time of 1 ms and can record temperatures up to 1832 degrees Fahrenheit. The probe was placed directly outside of the shock tube, where it would record flame temperatures of methane explosion with and without the addition of coal dust. The scaled shock tube was filled with methane gas, and sealed with a Styrofoam block. As in previously described testing, methane concentrations were monitored at various points along the length of the shocktube and coal dust was dispersed along the bottom at a concentration of 150g/$m^3$. The gas mixture was ignited using an electric match and the initial methane explosion created turbulence that also lifted and ignited the dispersed coal dust. The Optris temperature probe connects directly to a laptop via a USB port and uses independent software to record data, which can then be exported to Dplot for analysis. Figure 14 shows the placement of the temperature probe during this testing.

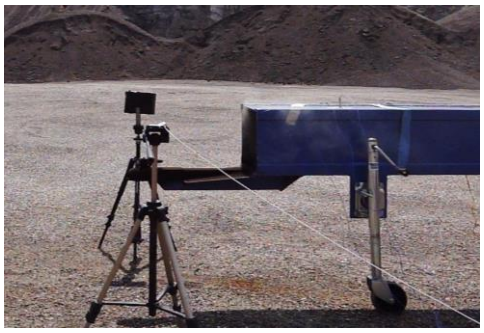

*Figure 14: Temperature Probe Setup*

As shown in Figure 15 and Figure 16 below, temperatures for methane only test peaked at 1108 degrees Fahrenheit. The addition of coal dust for these test increased the peak temperature experienced to 1494 degrees Fahrenheit.

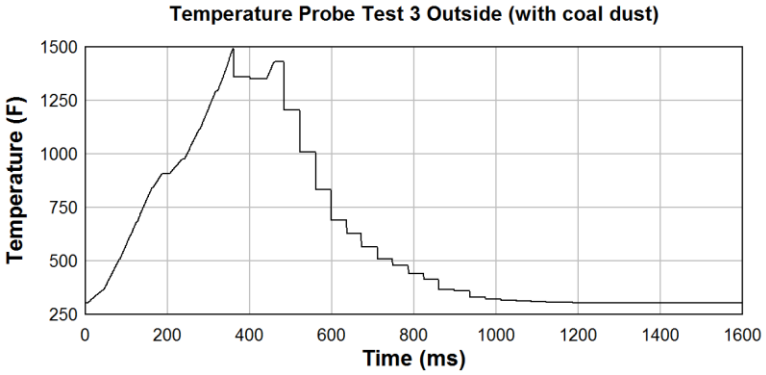


*Figure 15: Methane and Coal Dust Temperature Readings*

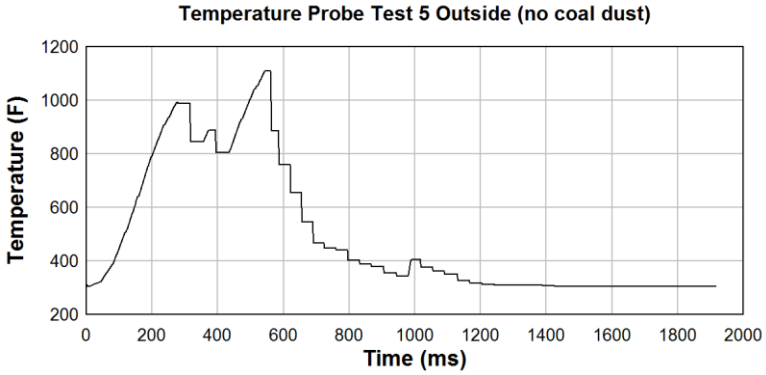


*Figure 16: Methane Only Temperature Readings*

Ultimately, three methodologies were explored by the UKERT team to protect against heat interference. Two involved a physical shielding structure to protect sensors from heat during an explosion and the third included a specially designed pressure sensor, manufactured to measure pressures in extreme atmospheres.

### *3.2.2 Method One: NIOSH Recommended Device*

Having decades of experience in explosion testing, NIOSH recommended the following device to the UKERT to help dissipate the heat created in an explosion before reaching the piezoelectric sensor. The rectangular mounting bracket, shown in Figure 17, houses a porous aluminum disc, which is designed to diffuse heat. The back of the mounting bracket is threaded to allow for the insertion of a pressure sensor.

*Figure 17: NIOSH Device*

### *3.2.3 Method Two: UKERT Fabricated Device*

Similar to the NIOSH recommended design, UKERT also fabricated a device designed to protect pressure sensors from high temperatures. Original designs included the use of invar, a material with a low thermal expansion. However, it was discovered that invar has a higher heat conductivity than steel. For this reason, the final design was crafted from steel, as shown in Figure 19.

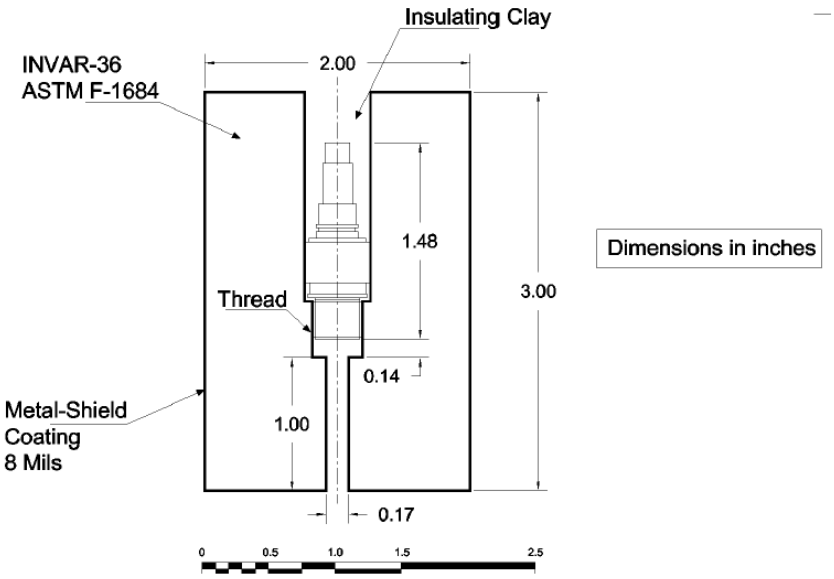


*Figure 18: Original UKERT Design*

*Figure 19: Final UKERT Design*

### *3.2.4 Method Three: Improved Pressure Sensors*

The third attempt to mitigate temperature interference focused on the pressure sensor itself. With the support of PCB Piezoelectrics, UKERT was able to test a 176M03 differential charge output sensor. The device, developed to record pressures in combustion engines, is much better suited for recording data in extreme conditions, such as those produced from exploding methane and burning coal dust.

*Figure 20: PCB 176M03 Pressure Transducer*

### *3.2.5 Testing of Three Methodologies*

Devices were originally tested inside the scaled shock tube. With limited access to mounting configurations, the devices were positioned in the upper corners of the shocktube. This resulted in noisy data due to the amount of pressure wave interference with the tube's 90-degree corners. It is hypothesized, that if the devices are mounted inside the full scale shock tube, the amount of open area will eliminate this interaction. Without access to a full scale shock tube, an alternative test was created to determine recommended shielding techniques for high temperature explosion testing.

It was crucial that each device be tested under identical conditions. To accomplish this, multiple mounting locations were created on a square steel plate. As shown in Figure 21, each mount is located 6 inches from the center of the plate. A side view shows that each shielding mechanism is mounted flush with the face of the steel. Additionally, the NIOSH recommended device is mounted in two locations, one which includes the rectangular aluminum bracket (denoted NIOSH_01) and one positioned directly in the steel without a mounting bracket (denoted NIOSH_02). This allows for any interference from the bracket

to be analyzed, with both locations still including the diffusive disc. As a baseline for measurements, two unprotected pressure sensors are also included. One is mounted in the center of the plate and the other along the outside of the configuration, six inches from the center (denoted PCB-01 and PCB-02). It should be noted that equivalent pressure sensors are used for each device, with the exception of the 176M03 device.

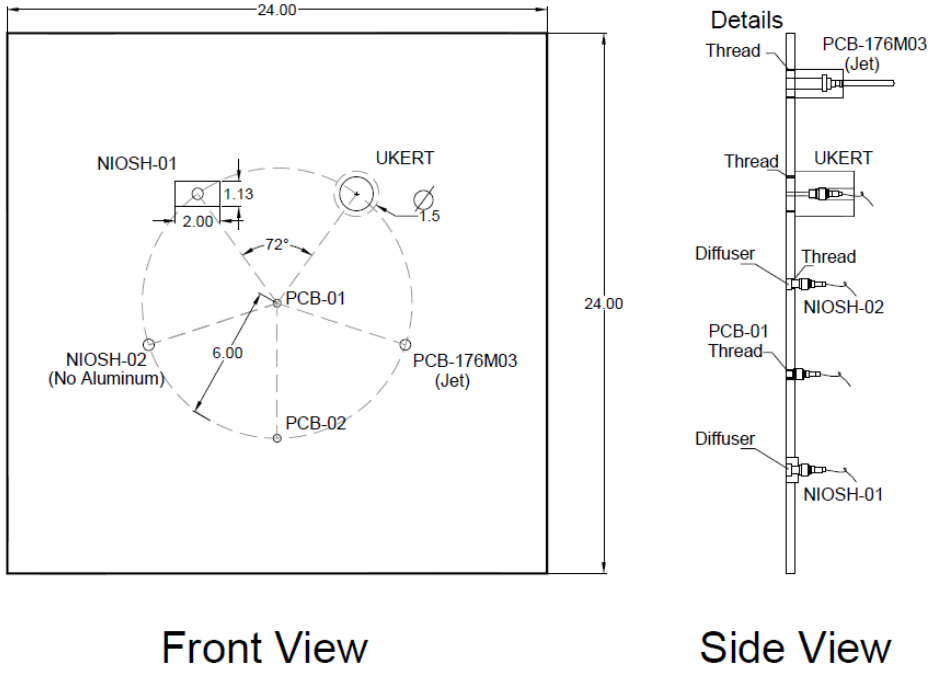


*Figure 21: Sensor Mounting Configuration*

The final plate construction is shown below. Small legs were welded onto each corner of the plate to support it in a horizontal position for testing.

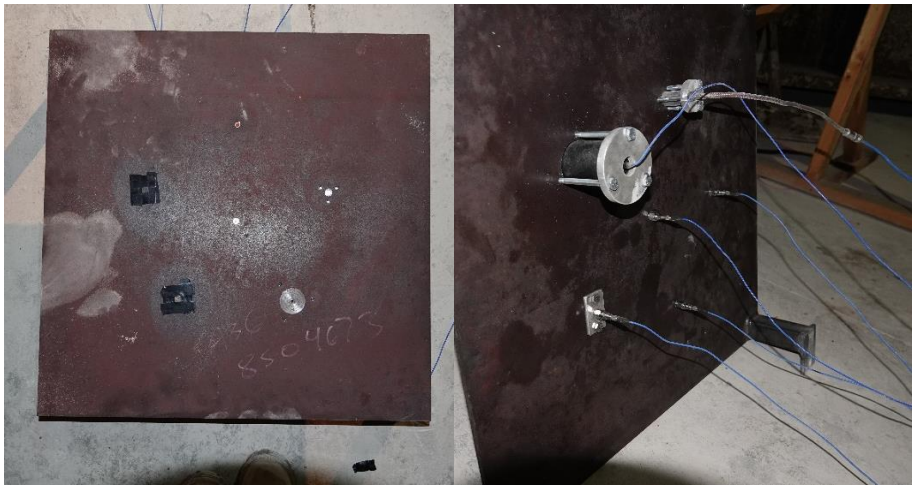

*Figure 22: Final Mounting Plate Configuration, Front and Back*

Because some of the mounting configurations reduce the exposed surface area of the sensors, a test was first completed to determine how the shielding assemblies would affect pressure readings. A shielding mechanism would only be considered successful if protected against heat interference and recorded accurate pressure readings. To determine the success of each method at these goals, two rounds of testing were completed.

Round one of testing exposed the sensors to a high explosive, with no potential for heat interference. A booster, filled with C-4, was located four feet above the horizontally positioned steel plate, as shown in Figure 23. Each sensor recorded pressure values during detonation, which could then be compared to the two unprotected sensors, which can accurately and reliably collect pressure data in the absence of heat.

*Figure 23: High Explosive Testing, Mounting Configuration*

A second test then determined how well each shielding mechanism mitigated the effect of heat in pressure readings. A coal dust and methane explosion was created in the scale shocktube following procedures previously described for testing of the temperature probe. The mounting plate was positioned vertically, outside of the shocktube, at a distance of 4-feet for Test 1 and 2-feet for Test 2. The results collected during this stage of testing can be found in Chapter four.

*Figure 24: Methane/Coal Dust Testing Setup*

It was important that different solutions be tested, to allow for recommendations for future work involving the measurement of pressures during methane and coal dust explosions. However, any further testing was not completed as a part of this thesis.

## 3.3 Multiple Detonations

Test completed to determine the potential of combining high explosive charges to alter pressure profile shapes, was completed using electronic detonators positioned inside the scaled shock tube in addition to two PCB pressure sensors as shown below.

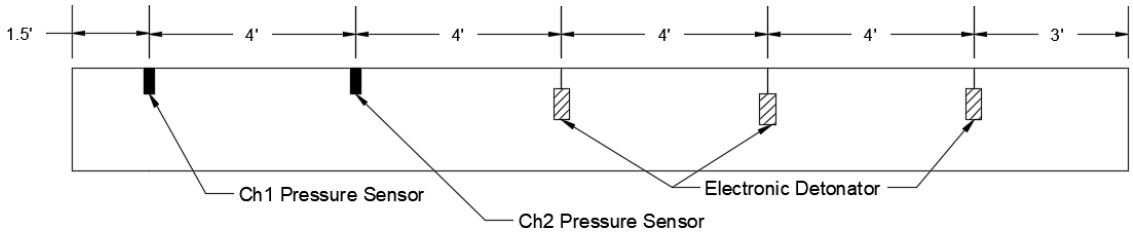


*Figure 25: Multiple Detonation Setup*

Using velocity of detonation values collected previously in high explosive testing, detonation delay times for testing using three charges were calculated. An initial test containing only one charge was completed to determine the peak pressure and impulse of a single detonator. Using an electronic detonation system, three charges were detonated in two additional test. The first test used a delay of 2ms between each charge and the second used a 1ms delay. The resulting pressure profile shapes, peak pressure and impulse values are provided in Chapter four.


*Figure 26: Electronic Detonation System*

# 4 Chapter 4: DATA COLLECTED

Chapter four presents the data collected during the series of test described in Chapter three. Basic conclusions presented in the data are given while further detailed discussions of the results are found in Chapter six. Graphs shown here have been created to best display the phenomenon studied in testing while applicable raw data collected are included in Appendix I.

## 4.1 Pressure-Time Curves for High and Low Explosives

Pressure history results from the testing described in Chapter three are given below. Detonator tests were completed five times and an approximation of the cumulative curves is provided in Figure 27. Methane test were successfully completed four times, with an approximation of the cumulative curves provided in Figure 28. The representative curves for the detonator and methane test were used to model high and low explosive curves, respectively, in both the SDOF and FEA analyses.

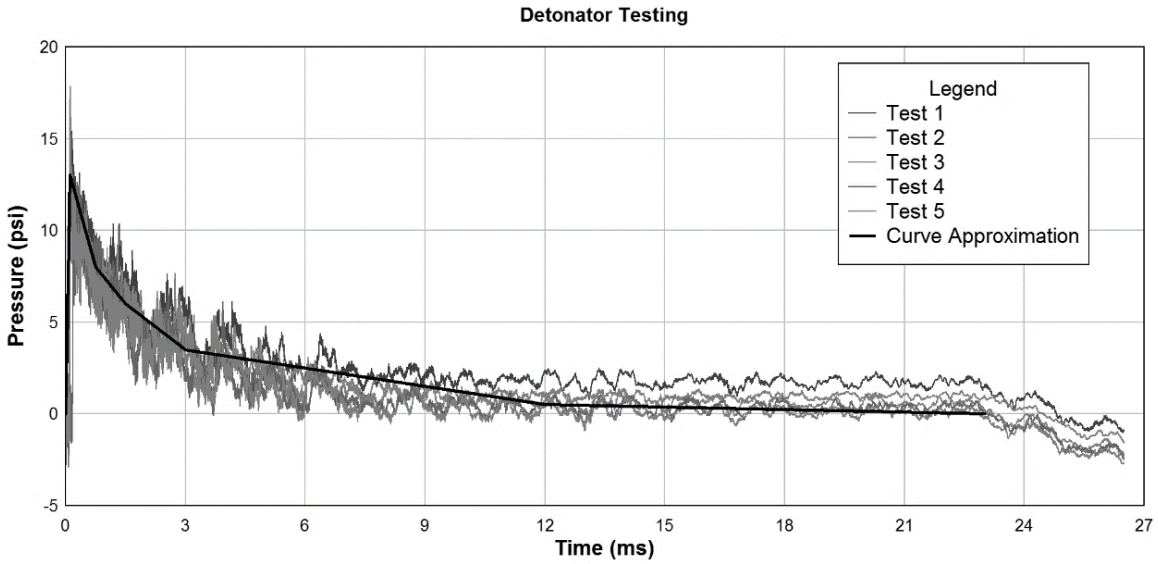


*Figure 27: High Explosive Pressure Histories*

The representative curve in Figure 27 is typical of a high explosive. The total duration of the positive impulse is 21 ms, the average peak value is 13 psi, which occurred at 1 ms. For this series of tests, the average impulse was 40.6 psi-ms. To simplify the structural analyses completed in this thesis, only the positive phase of the pressure curve is considered. However, the negative phase could be critical for the analysis of specific structures.

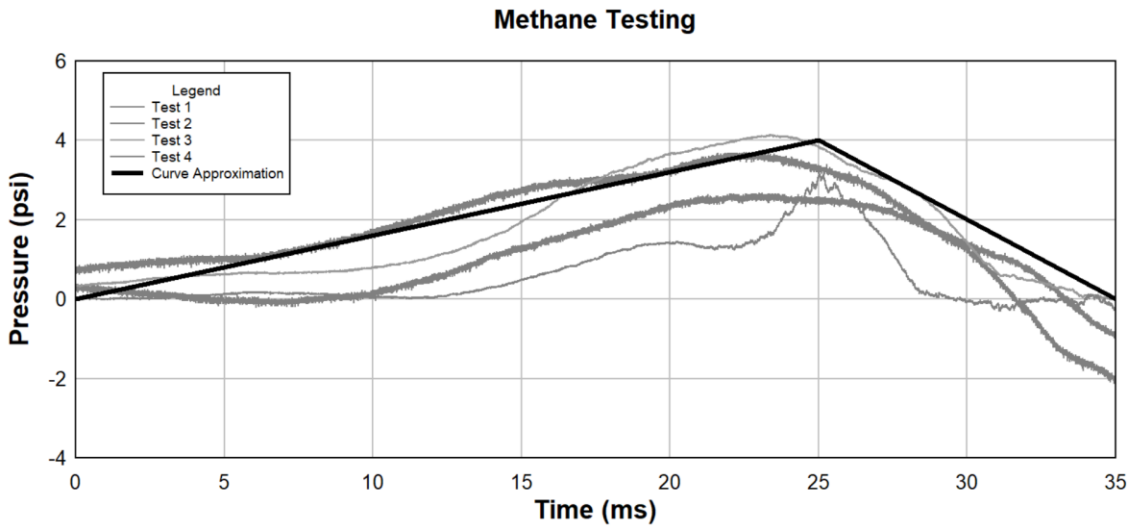


*Figure 28: Low Explosive Pressure Histories*

The representative curve in Figure 28 is typical for a low explosive charge. The total duration of the positive impulse here is 35 ms, the peak average value is 3.9 psi, and it was recorded at approximately at 24 ms. The impulse value, in this case, was 70 psi-ms.

When comparing the two sets of experimental data, relationships between peak pressure and impulse can be examined. Even though the low explosives had a peak pressure less than one-third that of the high explosive (3.9 psi to 13 psi), the average impulse values for the low explosive were almost twice those of the high explosive (70 psi-ms to 40.6 psi-ms). The importance of this relationship becomes critical when analyzing how structures will deform and move during an explosive event. This distinction is highlighted in future chapters.

## 4.2 Pressure-Time Curves from Heat Mitigating Methods

Pressure histories recorded while determining which methodology best produced accurate data during high temperature events is included below. The first series of results, shown in Figure 29, act as a control for determining if the mounting configurations under-represent or over-represent pressure readings. Three rounds of tested were completed, with results averaged for each method and shown below in Figure 29.

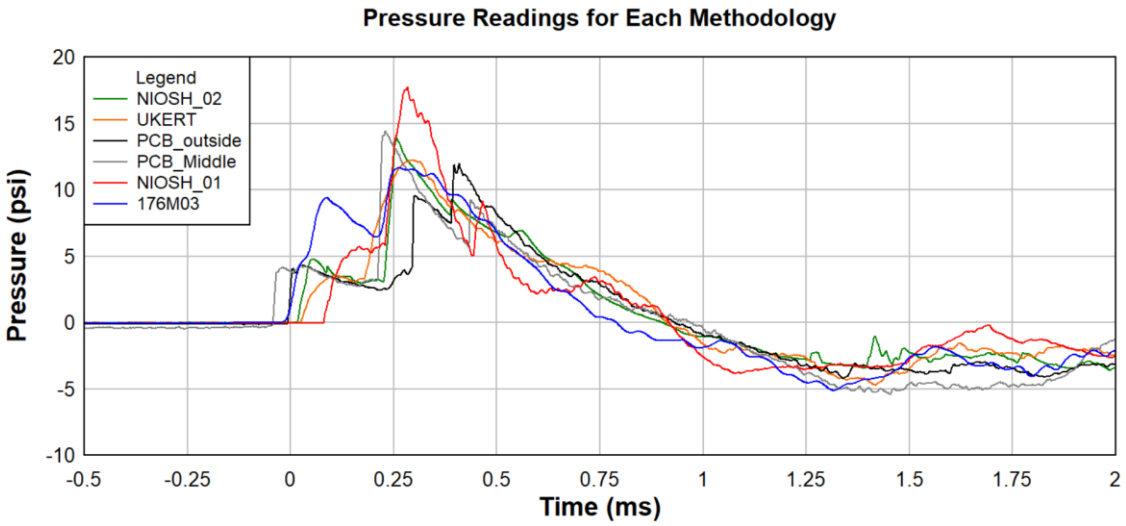


*Figure 29: Results From Pressure Configuration Testing*

In comparison to the two unshielded PCB sensors, shown in black and grey, all other pressure readings can be evaluated. Each pressure sensor was able to record the same general trend and standard high pressure wave shape. NIOSH_01 denotes the NIOSH recommended mounting in its original aluminum mounting bracket. This configuration recorded the highest peak pressure value at 17.7 psi, which is approximately 4 psi higher than the 13.8 psi average. NIOSH_02 produced similar wave shapes and pressure values to the two PCB pressure sensors. The 176M03 device also recorded similar peak pressure values, and captured the overall wave shape of the event. The UKERT recommended device appeared to deafen the pressure readings, as its pressure profile has rounded peaks, but does have comparable pressure readings. Overall, each pressure sensor was able to record similar data for the explosive event. While some shielding techniques resulted in slightly higher pressure values, none appeared to dampen the pressure values significantly. While three rounds of testing were considered adequate to distinguish any possible pressure reading errors, there was not enough data to statistically discern if any pressure readings are statically different from the unshielded sensors. It was determined that each pressure sensor could accurately record pressure data, and a method's success would be dependent on how well it negated heat interference.

The second set of results from this portion of testing included each mounting configuration being subjected to a methane and coal dust explosion. Two rounds of testing were completed. In round one, the steel plate was positioned 4-feet from the end of the shock tube. In round two, the plate was moved closer, positioned 2-feet from the end of the shock tube. As expected, the large amount of heat produced during this explosion caused both unprotected PCB sensors to produce erroneous data. However, it was not expected that the 176M03 sensor would produce similarly inaccurate data. For this reason, data from these three sensors are not included in the following plots, but can be found in Appendix I. The

resulting pressure readings for both NIOSH sensors and the UKERT sensor for Tests 1 and 2 are shown below in Figure 30 and Figure 31.

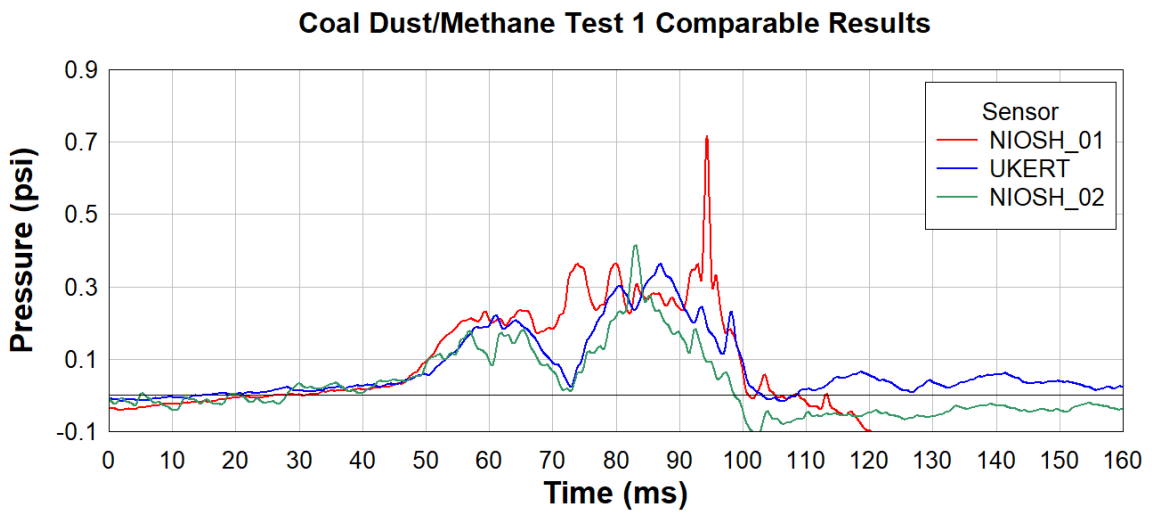


*Figure 30: High Temperature Test 1Pressure Readings*

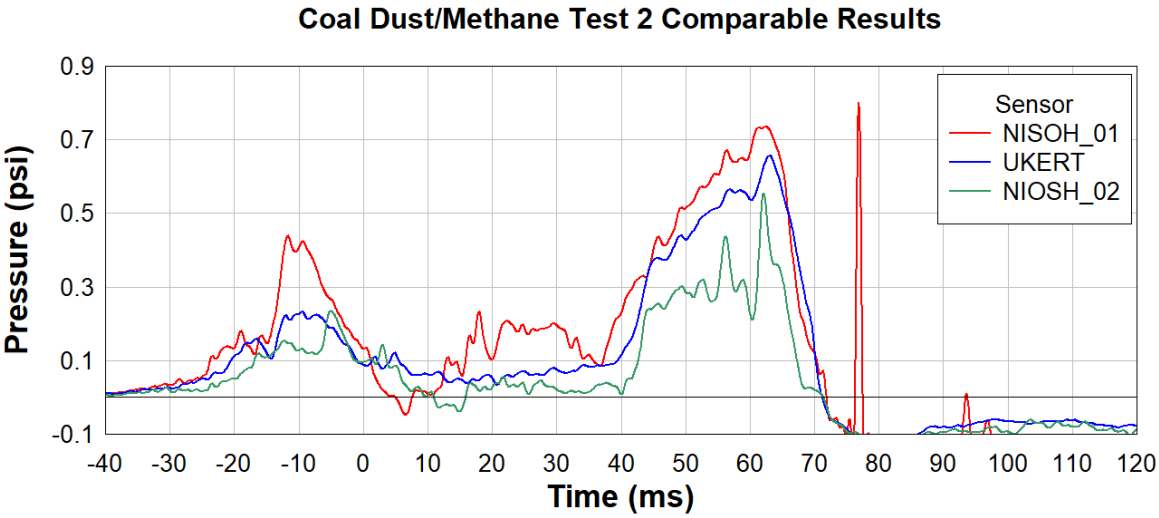


*Figure 31: High Temperature Test 2 Pressure Readings*

As these sensors are positioned outside of the shock tube in addition to the lower pressures expected from a methane/coal dust explosion, the pressure readings here are not as significant as the profile shapes recorded. While none of the graphs match exactly, similar wave shapes were recorded from each sensor. It should also be noted, that unlike high explosive testing, no two methane and coal dust test will ignite in exactly the same gas to dust ratios. The resulting pressure wave created is less uniform than with high explosives and can produce unequal areas of heat and pressure. To help reduce this interference, sensors were mounted in a circular pattern at an equal distance from the end of the shocktube, however all differences in pressure wave and flame front cannot be accounted for.

## 4.3 Pressure-Time Curves for Multiple Charges

Figure 32 shows the resulting pressure profiles recorded after the detonation of a single electric detonator in the scaled shocktube. Two pressure sensors were mounted, as described in Chapter two, and are shown in as channel one and two.

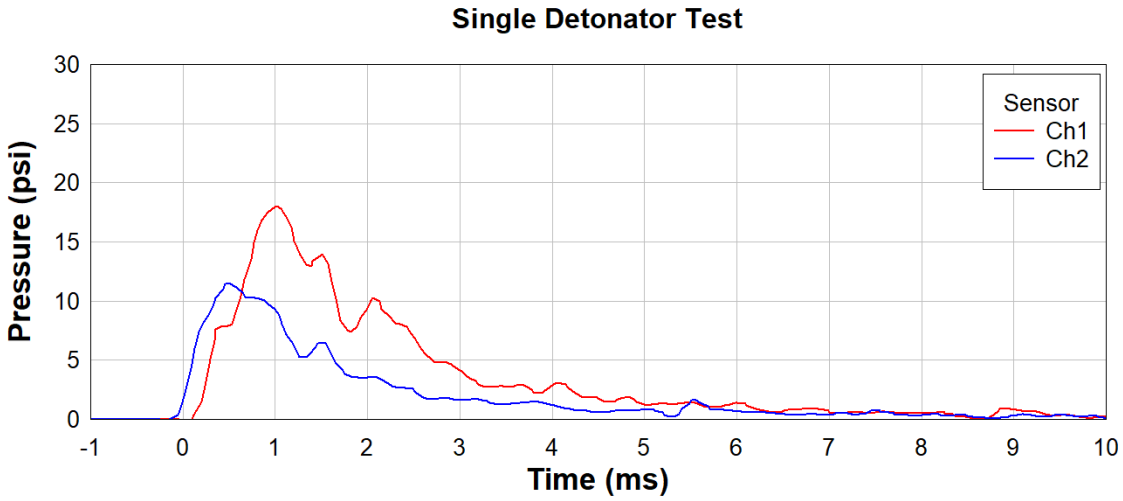


*Figure 32: Pressure Curve for Single Detonator*

Figure 33 shows the resulting pressure profiles recorded after the detonation of three electric detonators in the scaled shocktube, with a delay time of 2ms between charges. Here, three distinct peaks can be distinguished within the overall profile, corresponding to the three detonators. Figure 34

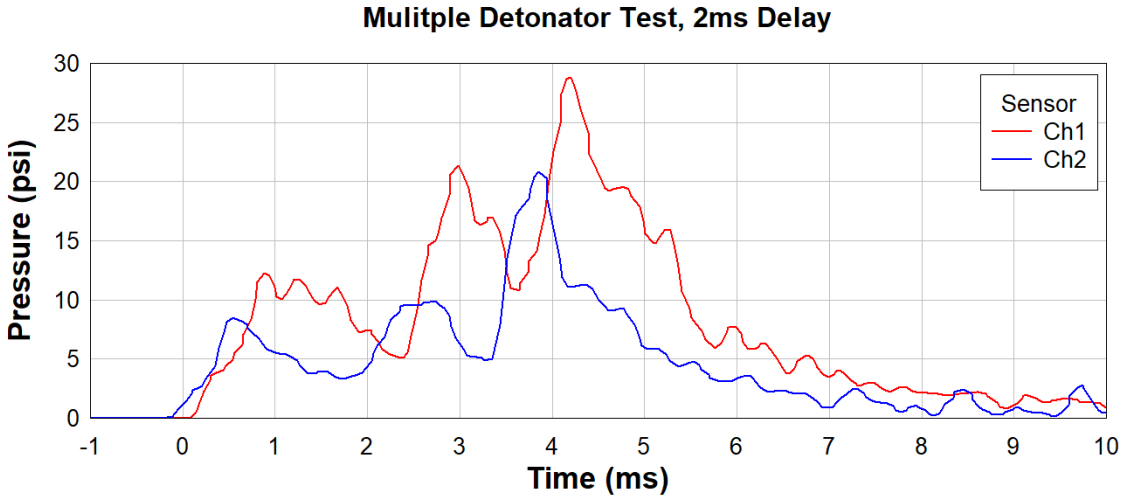


*Figure 33: Pressure Curve for Multiple Detonators at 2ms Delay*

Figure 34 shows the resulting pressure profiles recorded after the detonation of three electric detonators in the scaled shocktube, with a delay time of 1ms between charges. Here, the three distinct peaks are harder to distinguish in the overall profile.

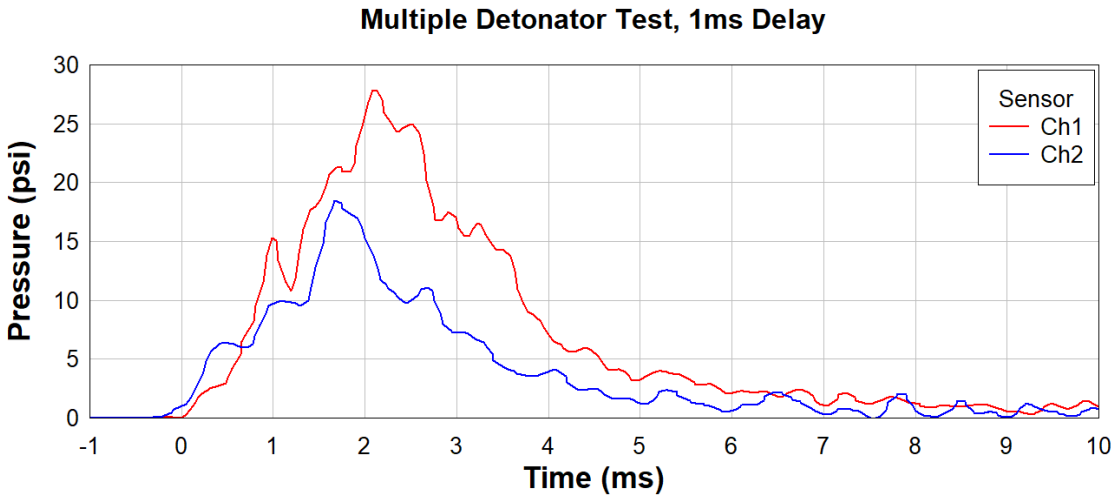


*Figure 34: Pressure Curve for Multiple Detonators at 1ms Delay*

Peak pressures and impulse values for each test are provided in Table 2 below. It is shown that the peak pressure values are not significantly different between the 2ms and 1ms testing. However, with the increase in overall pressure duration, the impulse values for both test involving three detonators is significantly higher than the single detonator test.

*Table 2: Peak Pressure and Impulse Values*

| Test | Ch. | Peak (psi) | Impulse (psi-ms) |
|---|---|---|---|
| **Single** | 1 | 18.1 | 35.3 |
| | 2 | 11.5 | 21.5 |
| **2ms Delay** | 1 | 28.8 | 92.2 |
| | 2 | 20.8 | 56.0 |
| **1ms Delay** | 1 | 27.8 | 75.5 |
| | 2 | 18.4 | 45.8 |

# 5 **Chapter 5:** STRUCTURAL ANALYSIS

Chapter five explores different approaches to study the response of structures to different pressure waves. The complexity of approaches increases, building on the findings of the previous cases allowing for the completion of more detailed analyses.

## 5.1 Single Degree of Freedom System Analysis

As previously described, a single degree of freedom (SDOF) structure was selected to initially analyze the effects of contrasting pressure profiles on underground mine structures. The parametric study implemented pressure profiles described in Chapter four to determine the displacement of an elastic rectangular cantilever beam with damping applied. A detailed analysis of SDOF structures under dynamic loads can be found in Biggs (1964). Biggs (1964) provides, a detailed procedure to solve the partial differential equations governing the behavior of SDOF structures, using numerical methods (finite differences).

Figure 35 shows the idealized spring-mass system used for the SDOF analysis. The weight and the spring constant must be selected to accurately represent the deflections of actual structures. Here, the constant $k$ is the ratio of force to deflection of the beam. Additionally, to make the model more realistic, damping was considered, where $c$ is the damping constant. Lastly, $y$ represents the displacement of the mass $M$. The SDOF system shown in Figure 35 (a) can be drawn as the free body diagram shown in (b).

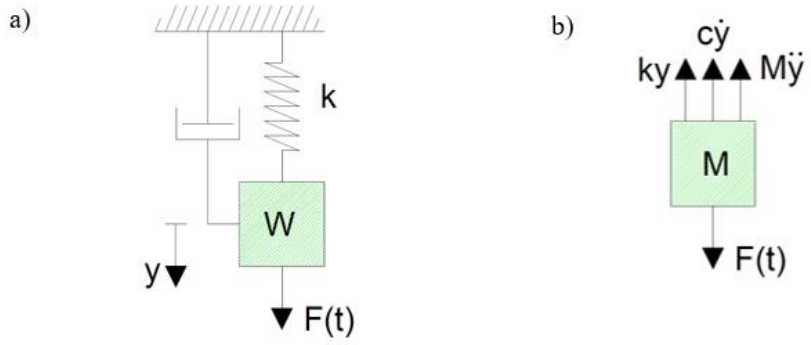


*Figure 35: Damped Spring Mass System: a) System; b) Forces acting in the free body (Adapted from Biggs 1964)*

Using Newton's second law of motion, Equation 3 describes the motion for the system under analysis.

$$F(t) - ky - c\dot{y} = M\ddot{y}$$

*[3]*

A finite difference scheme can be used to solve Equation 3, where the unknown variables are: velocity ($\dot{y}$), acceleration ($\ddot{y}$) and displacement ($y$). The recurrence equations are included as Equations 4 to 6.

$$\dot{y} = \frac{y - y'}{\Delta t} + \ddot{y}\frac{\Delta t}{2}$$

*[4]*

Where $y'$ denotes the previous position. Combining equation [3] and [4], the following equation is obtained for the acceleration,

$$\ddot{y} = \frac{F(t) - ky - c(y - y')/\Delta t}{M + c\Delta t/2}$$

[5]

The acceleration at every time step can be estimated using equation [5]. This value is necessary for calculating the position at subsequent time steps, which ultimately is the entire purpose of this process.

$$y = 2y' - y'' + \ddot{y}'(\Delta t)^2$$

[6]

Finally, the time step $\Delta t$ is assumed to be less than one-tenth the natural period $T$. The natural period can be calculated using the following equation.

$$T = 2\pi\sqrt{\frac{W}{kg}}$$

[7]

At this point, equations [5] and [6] can be solved simultaneously. This process begins with the assumption that the starting velocity ($\dot{y}$) of the structure is zero, and that the acceleration at time zero can be used in the following equation to provide the position at the first time step.

$$y_{t1} = \frac{1}{2}\ddot{y}_{t0}\Delta t^2$$

[8]

This process continues for some iterations until the desired time duration of the load is completed. The calculations of the displacement of the structure during an explosive event, can be done using equations 4-8, where the varying force $F(t)$ is equal to the pressure

histories recorded. For this initial analysis, it was assumed that the pressure that would be equally loaded over the face on an object was applied as a point source. Later analyses exclude this assumption and consider pressure loading.

Figure 36 includes both the applied force, which derives from the representative curve determined from the methane testing and the predicted displacement.

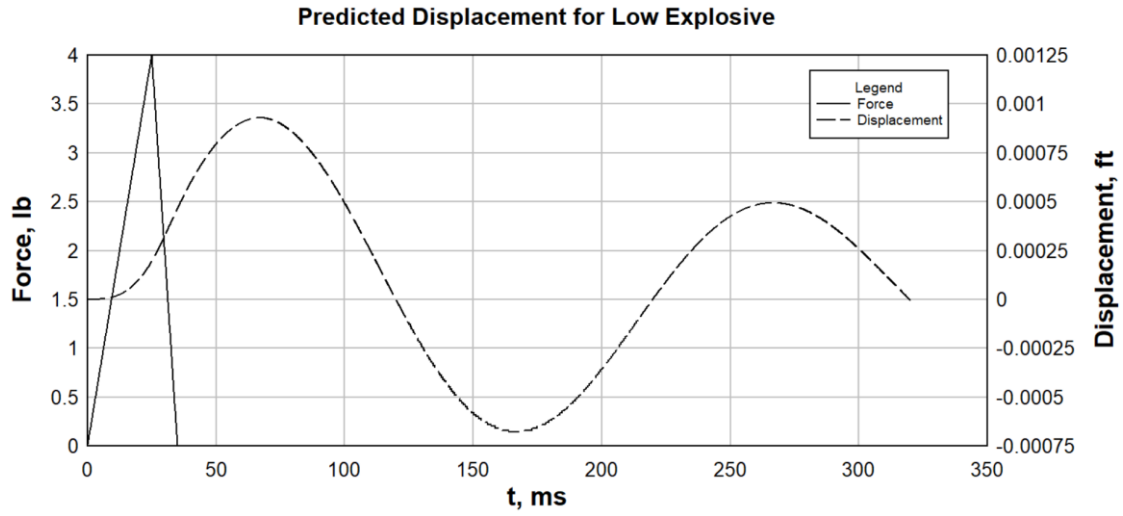


*Figure 36: Predicted Displacement from Low Explosive using SDOF Method*

This process was also completed for the representative curve for the high explosive. The results of this analysis are shown below in Figure 37.

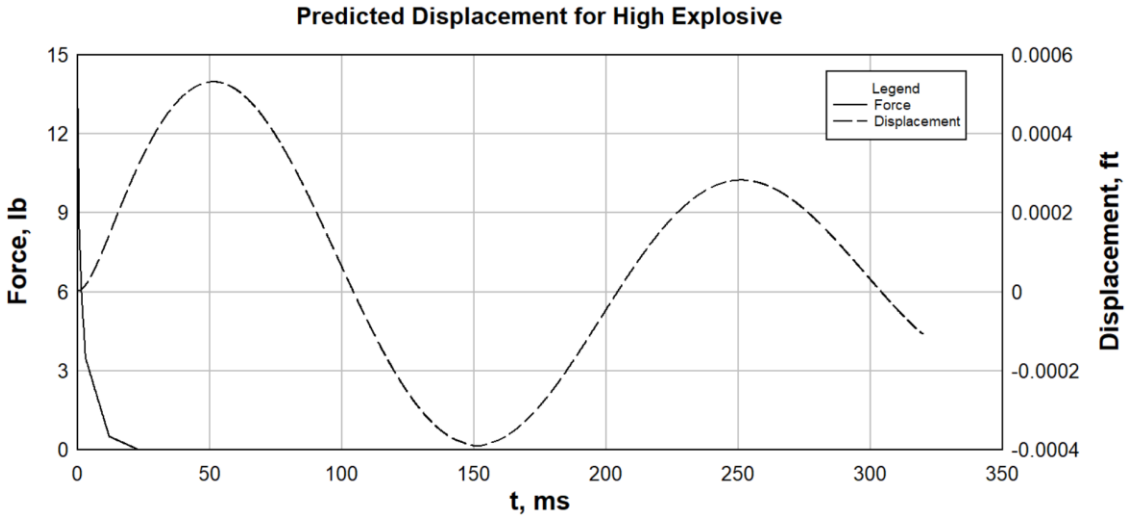


*Figure 37:Predicted Displacement from High Explosive using SDOF Method*

The manual calculations using finite differences were completed for both the high and low explosive cases for a time duration of 300 ms. This allowed for one cycle of the periodic oscillation to be shown, while also displaying the impact of damping with the second peak

displacement being lower than the first. This exercise was completed to understand the fundamentals of structure displacement under dynamic loading, and to contrast any differences between the two loading functions. Because no specific physical structure was being represented by this analysis, constant values for both cases were given as:

*Table 3: SDOF Units*

| | |
|---|---|
| $k$ | $2000\ lb/ft$ |
| $weight$ | $64.4\ lbs\ \therefore M = 2$ |
| $c$ | 0.1 |

## 5.2 Finite Element Analysis for a Beam

Building on the results from the finite differences method, further research in structural deflection was completed using the Finite Element Analysis software MSC Marc. MSC Marc was chosen as a tool for analysis because it is a powerful, general-purpose, nonlinear FEA software used to simulate the response of objects under dynamic loading scenarios.

A previously studied cantilever beam example was used as the framework for initial work completed in MSC Marc and is shown in Figure 38.

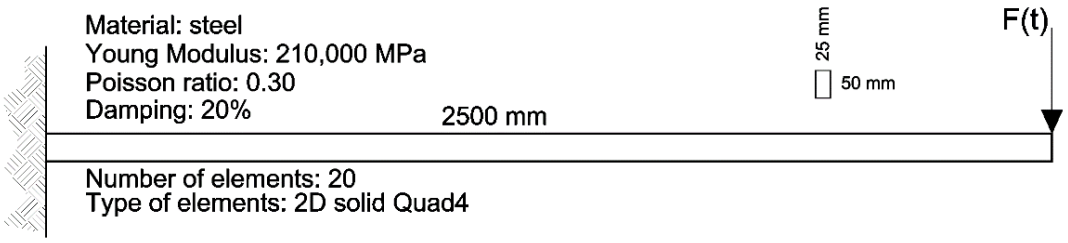


*Figure 38: Beam Used in Analysis*

Four cases were studied using the beam, each chosen to represent a specific phenomenon associated with the influence of profile shape on structural displacements. These cases show the influence and magnitude of key phenomenon to be used in further models.

*Table 4: Beam Case Studies*

| Case | Phenomenon Studied |
|---|---|
| 1 | High explosive loading versus low explosives loading |
| 2 | Quasi-static loading versus low explosive loading |

| | |
|---|---|
| 3 | Profile shape of high and low explosive with same impulse |
| 4 | Importance of rise time for equal maximum loading |

### *5.2.1 Case One: High versus low explosive loading*

As with the finite differences method, a simplification was made by converting pressure to a point source. This was done assuming the pressure was applied to an area of 5.51 $in^2$, which scales the peak pressure for the low explosive to a value of 22.04 lb (10 kg). This value was chosen because MSC software works primarily in metric units. This same scaling was also applied to the pressure-time curve used to describe a high explosive event. Figure 39 shows that the waveform is preserved through this units conversion, and only pressure values are altered. This exercise was not completed to represent a specific event, but rather to highlight differences between the two load cases.

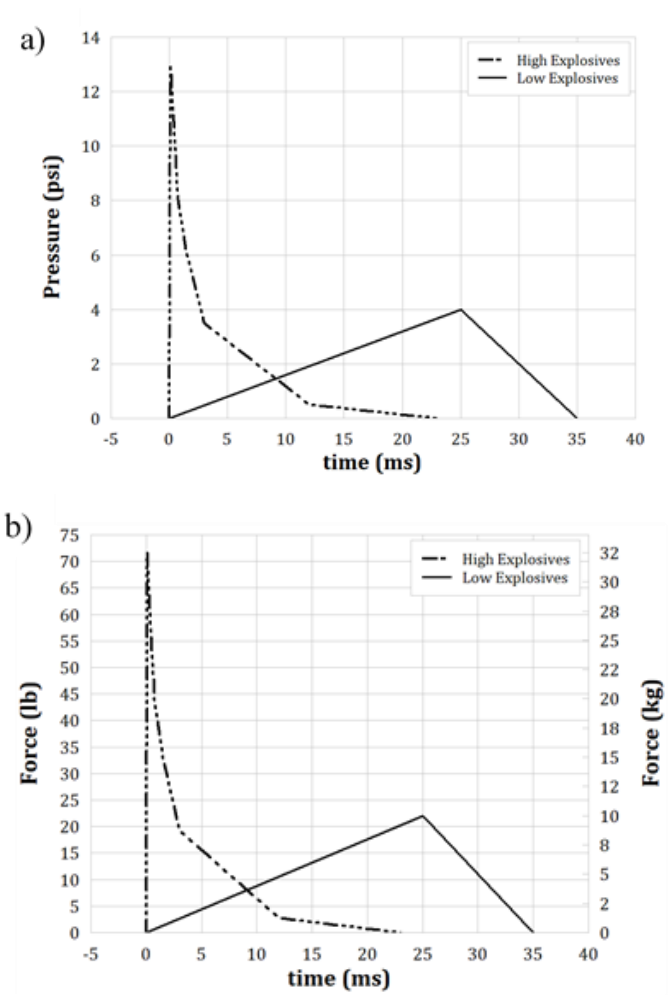


*Figure 39: a) Pressure profiles; b) Force profile for analysis*

Using the pressure profiles shown above, and the material and loading conditions found in Figure 38, an analysis was ran in MSC Marc for a total time of 1 second, with a time step of 0.001 second. The resulting displacement of the beam for this scenario is shown below in Figure 40.

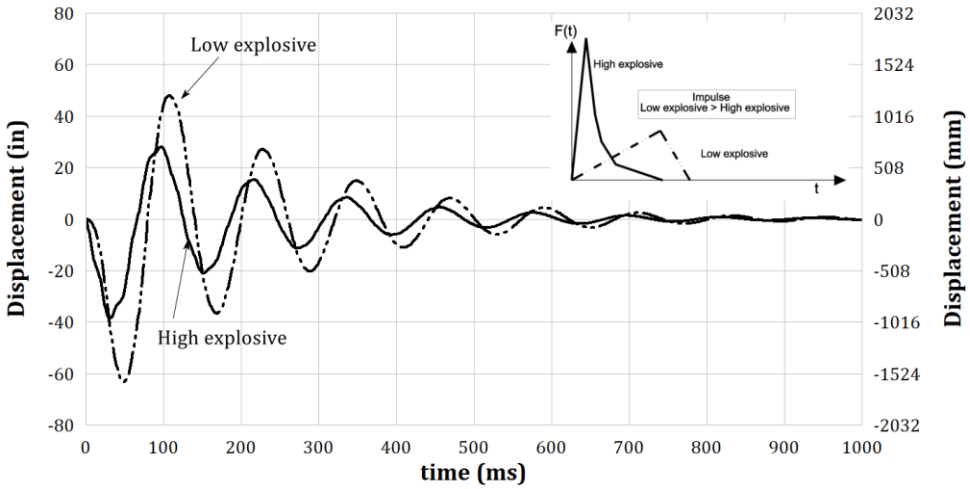


*Figure 40: High vs Low Explosive Displacement*

While the high explosive has a peak pressure three times that of the low explosive, the low pressure produced a larger displacement.

### *5.2.2 Case Two: Quasi-static versus low explosive loading*

As previously shown, the profile shape of a low explosive resembles a triangle with increasing pressures to a singular peak pressure, followed by decreasing pressures. However, some design guidelines include design profiles with constant loading at time zero and no specified duration. To analyze the effect of this quasi-static loading situation, the following profiles, included in Figure 41, were studied. As with case one, the peak pressure for both profiles was kept as 10 kg.

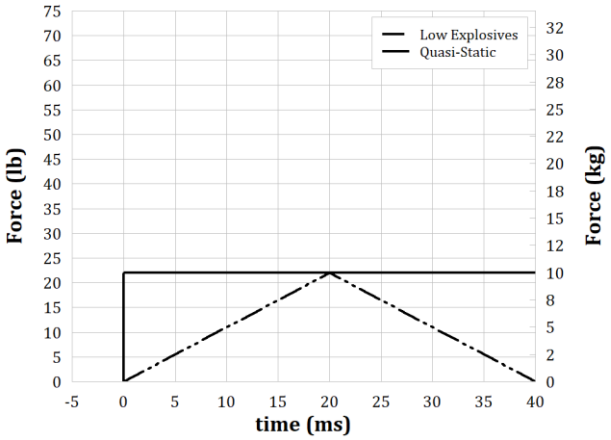


*Figure 41: Quasi-static and Low Explosive Loading*

The resulting displacement profiles for the loading functions in Figure 41 are given below in Figure 42.

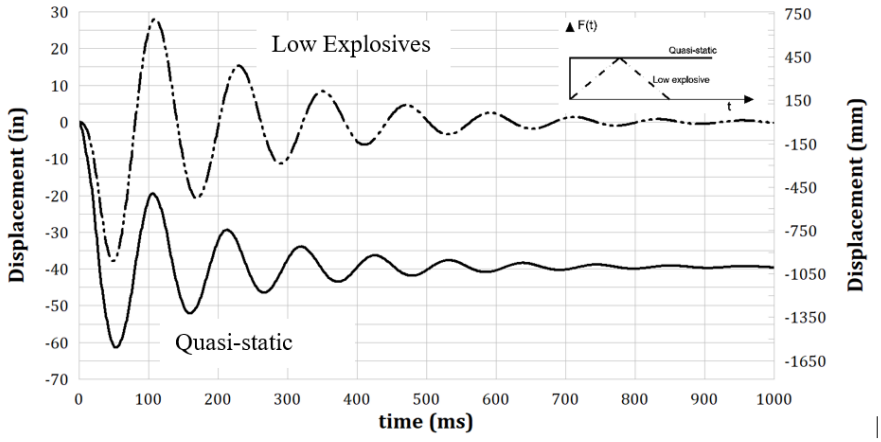


*Figure 42: Quasi-static vs Low Explosive Displacement*

For the quasi-static condition, there is a permanent displacement after the load is applied. Additionally, after initial oscillations damper out, the profile of the displacement plot becomes similar to the loading plot. Here, the quasi-static load resulted in a higher displacement.

If the quasi-static load is removed after some time, the beam will respond dynamically with displacements similar to that of the low explosive, as shown in Figure 43.

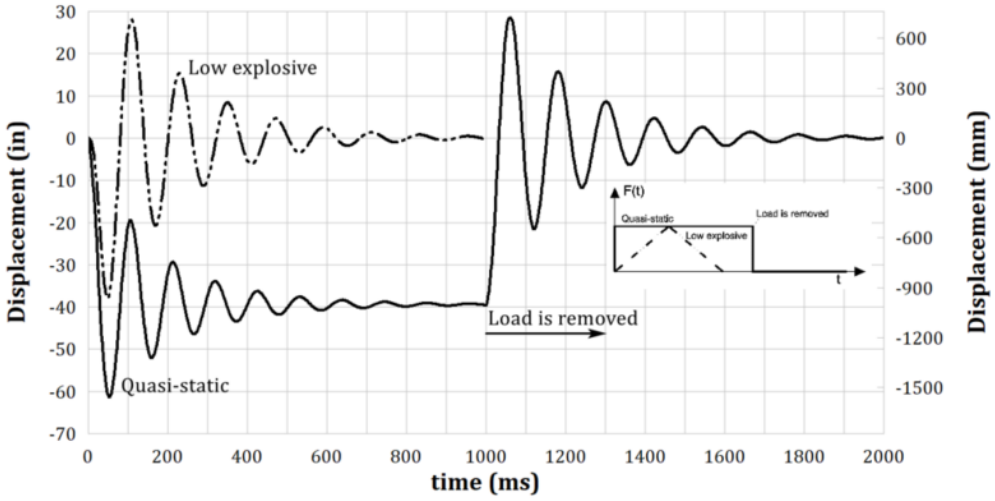


*Figure 43: Removal of Quasi-static Loading*

### *5.2.3 Case Three: High versus low explosive profiles with equal impulses*

If wave profile shapes could be manipulated by using multiple low explosives in laboratory environments, more realistic testing conditions could be achieved. The profiles shown in Figure 44 were chosen to evaluate the influence of the combination of both impulse and wave shape. Here, profile shapes were modeled from data collected during testing and a peak value of 10 kg of force was given to the low explosive curve. The peak of the high explosive curve was scaled to 125 kg to have the same impulse value of 200 kg-ms.

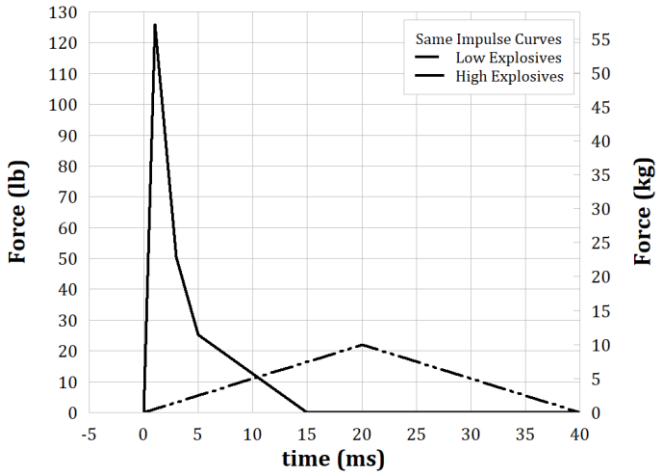


*Figure 44: High and Low Profiles with Equal Impulse Values*

While wave shapes for the high and low explosive are comparable to those used in case one, manipulating the profiles to have equal impulse values causes the displacement plots to become much more similar.

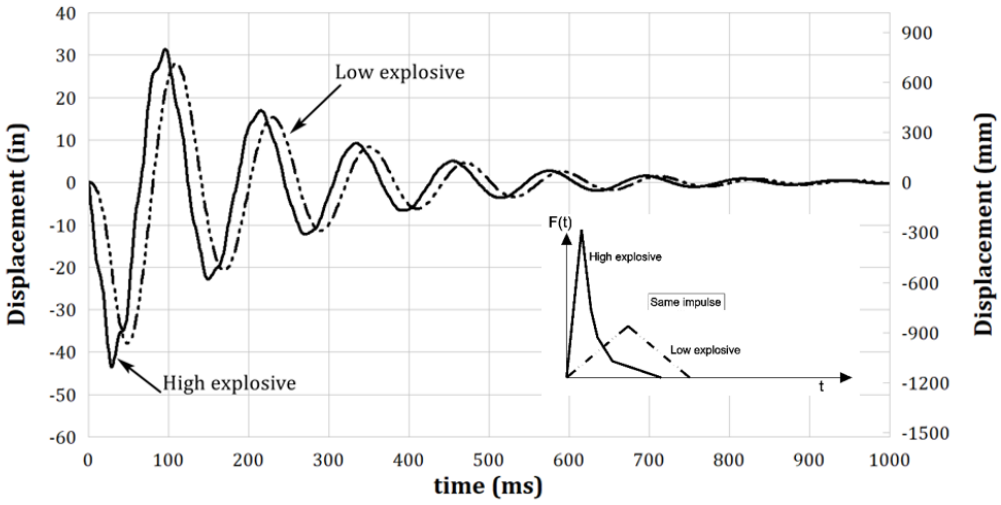


*Figure 45: Displacements for Equal Impulse Loading*

### *5.2.4 Case Four: Influence of Rise Time*

In all previous cases, the duration of the loading function was less than 40 ms, with the rise time to peak pressure values being less than 20 ms. However, as with the research completed by Sapko et al. (2008), it was discovered that increasing rise time forces displacement functions to more closely resemble the profile of loading function, with oscillation motion being minimized. According to NIOSH recommendations, designs should withstand loading moving from 0 to 120 psi in 250 ms. The resulting displacement from this loading is shown as the solid black line in Figure 46. Decreasing this rise time to values of 100, 50, and 0 ms, increases the maximum displacement of the beam while also increasing the amplitude of oscillations, which is also shown in Figure 46.

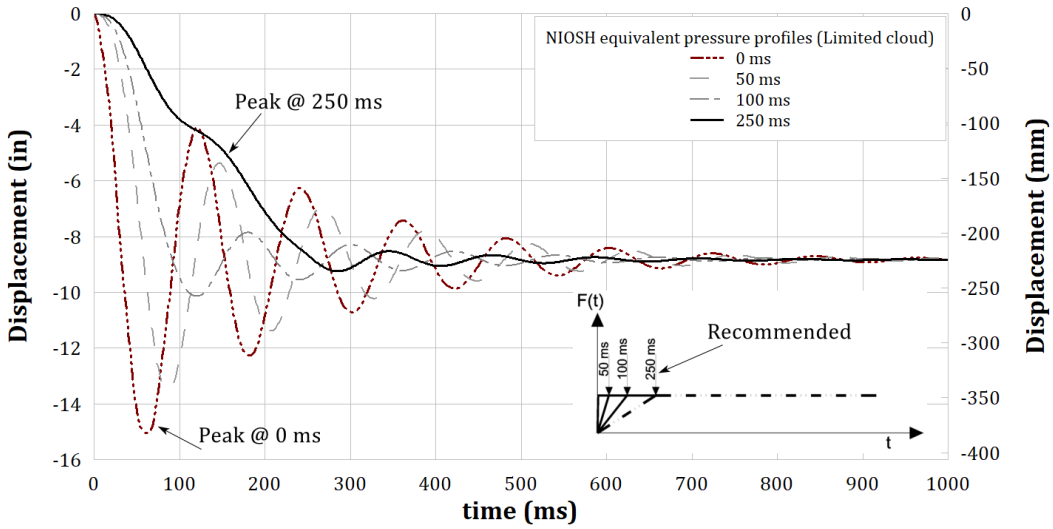


*Figure 46: Displacements from Various Rise Times*

## 5.3 Calibration of Model

The beam example was used as a calibration tool to create more realistic geometries and loading scenarios. A wall, measuring 2.5 x 2.5 m was created. As with the beam, the wall was restricted on one edge and was given a thickness of 50 mm. The material characteristics listed in Figure 38 were also used. The loading applied to the wall however, was implemented as a pressure rather than a point force. For both scenarios (beam and wall) the same loading function was applied and is given below.

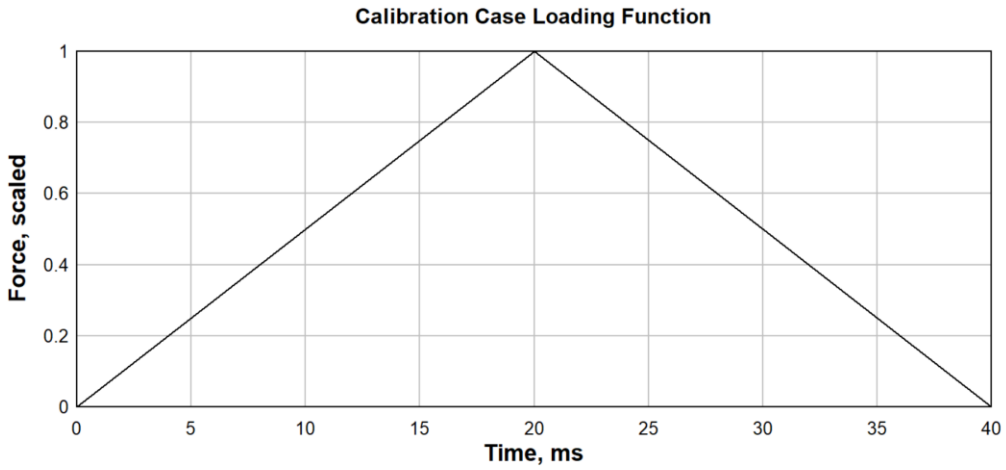


*Figure 47: Calibration Loading*

The simple loading function used to calibrate the model had one peak value which occurred at a time of 20 ms. Analyses were completed for a total time of 1 second, with no forces/pressures being applied after a time of 40 ms. Within MSC Marc, loading functions are given with the peak force/pressure scaled to a value of one. Within the analysis, pressure/force values are entered to represent specific cases. For calibration, a pressure of 120 psi was used.

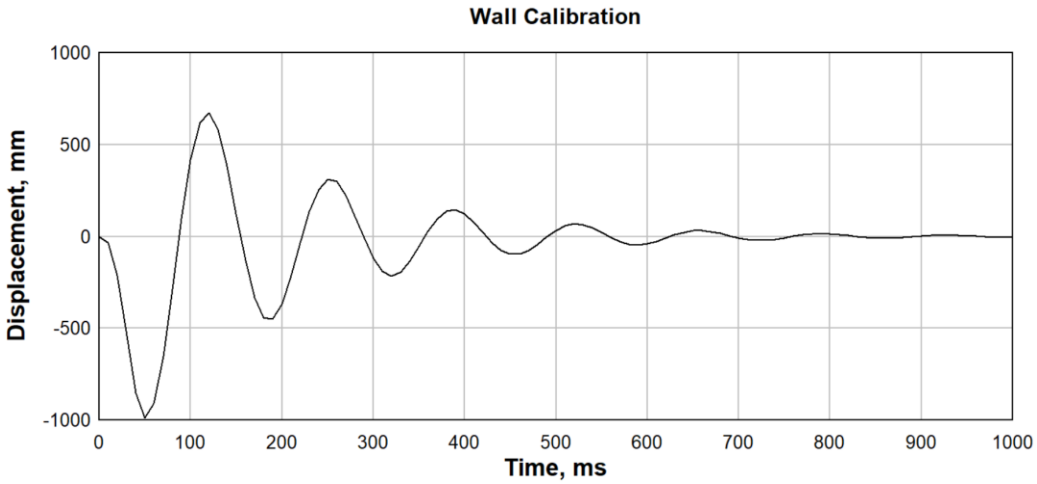


Figure 49 show the results from the calibration analysis, where both the beam and the wall show similar displacements over the same time frame.

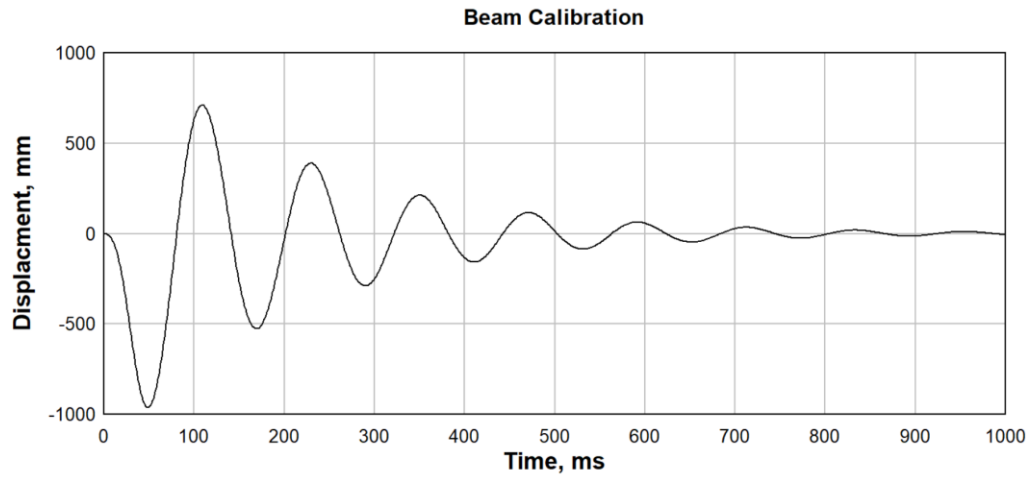


*Figure 48: Beam Displacement*

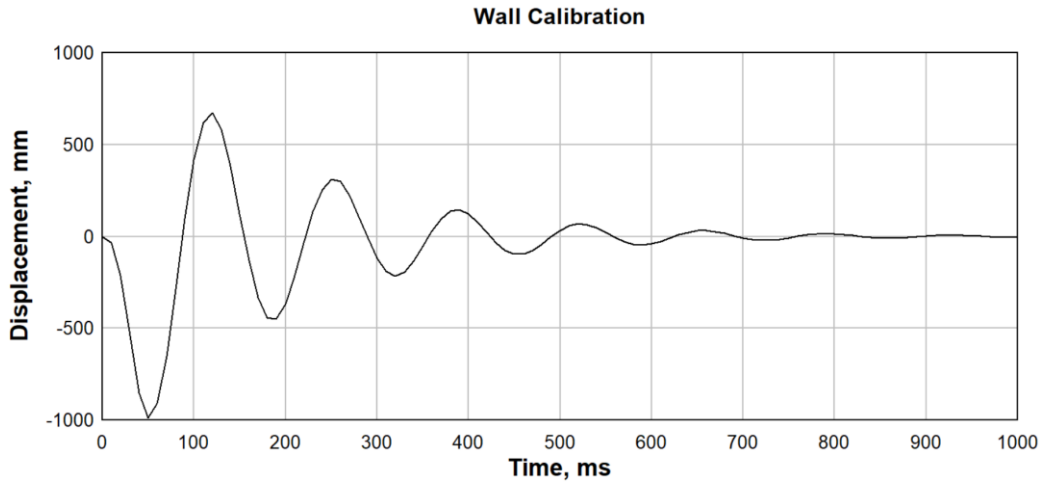


*Figure 49:Wall Displacement*

## 5.4 Studies with Mine Entry Geometries

Further FEA were completed using more realistic wall geometries. Reflecting the height and width of a typical room-and-pillar coal mine entry, as shown below, a width of 6 m and a height of 1.5 m (20 ft x 5 ft) was chosen.

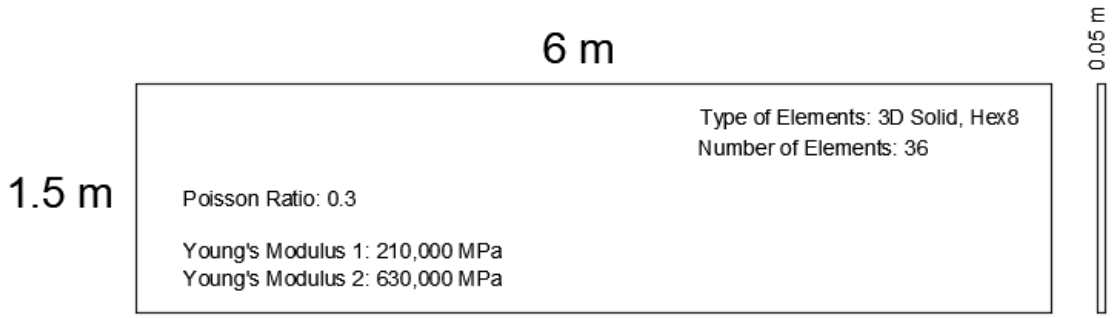


*Figure 50: Wall Geometry*

To compare further displacement plots, the wall geometry in Figure 50 was subjected to the calibration case loading function. As shown below in Figure 51, the increased wall width to height ratio dramatically decreases the displacement of a node positioned at the top of the wall.

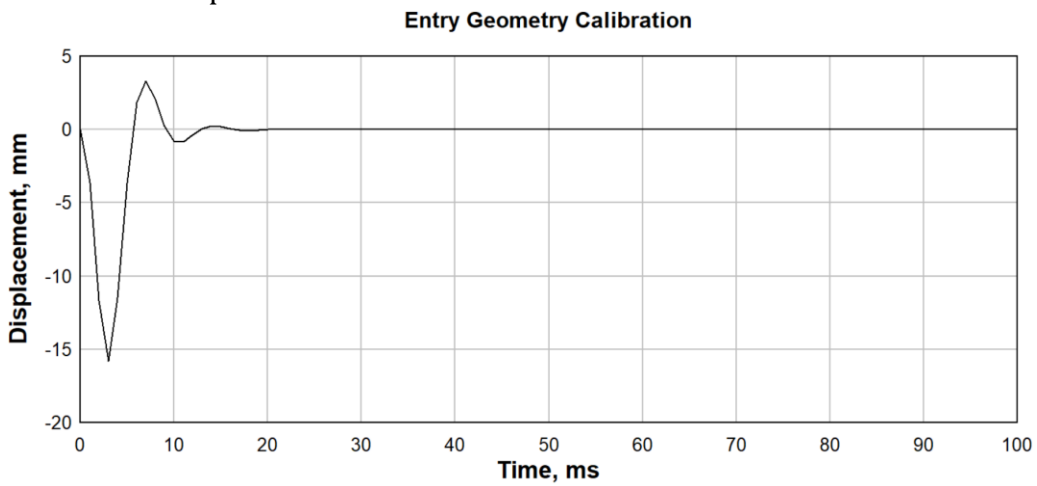


*Figure 51: Mine Entry Geometry Displacement for Calibration Loading*

Additionally, to better simulate actual mine seals, boundary conditions were changed to include all four sides being constrained, preventing boundary displacement. Two studies were completed using the entry geometry and new boundary conditions. Study one, compared the displacement of the wall during two specific pressure events. The first event was modeled after a standard design curve, previously used for mine seals. It has a duration of 200 ms and a peak pressure of 15 psi, as shown in Figure 52. The second event was modeled after the NIOSH recommended design curve, with a rise time of 25 ms and a peak pressure of 120 psi that extends for the duration of the study. The NIOSH recommended design curve is shown in Figure 53.

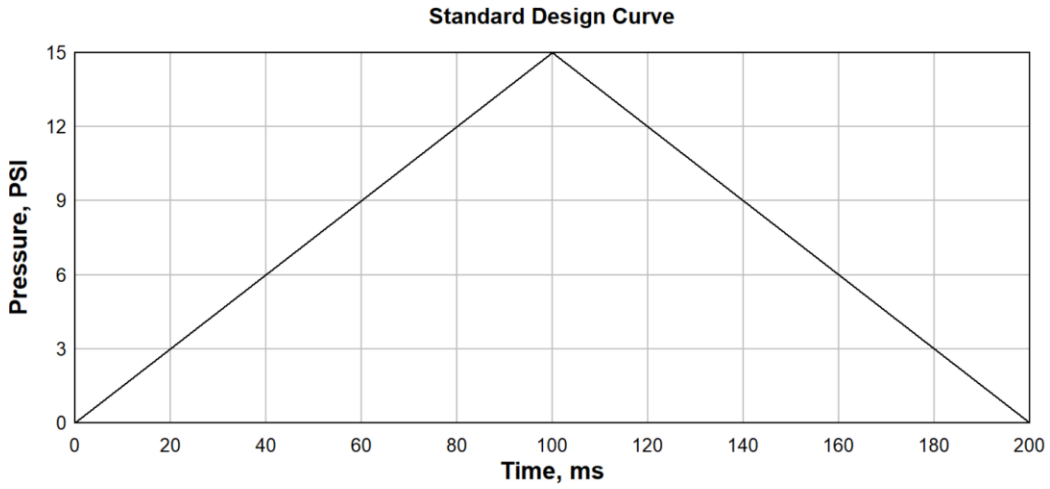


*Figure 52: Pressure-Time Plot for Standard Design Curve*

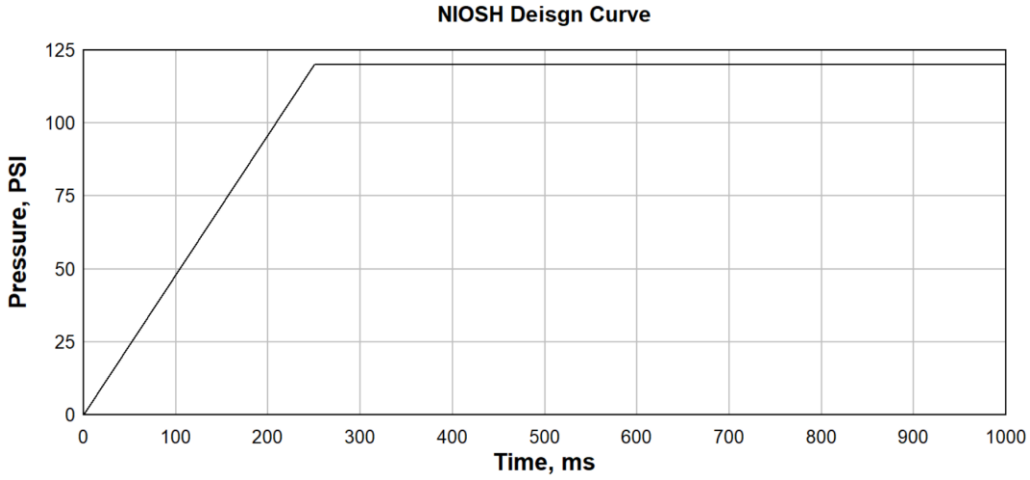


*Figure 53: Pressure-Time Plot for NIOSH Design Curve*

The second study is concept driven. Creating a model to accurately represent the various material layers and interactions within a mine seal involves many variables, not explored in this research. To replicate that process, Young's modulus of elasticity of the material used in the FEA is increased by a factor of three and the displacements compared. At some point, increasing the strength of a mine seal becomes futile when the pressure experiences overcome the bondage strength between the seal and the mine wall. In this study, stress conditions along the boundary of the wall are studied under the loading conditions of the standard design curve.

### *5.4.1 Study One Results*

As shown in Figure 54 and Figure 55, the displacements for both the Standard and NIOSH loading reflect the shape of the loading functions. Because the edges are bound, displacement values are taken from a node located in the center of the wall.

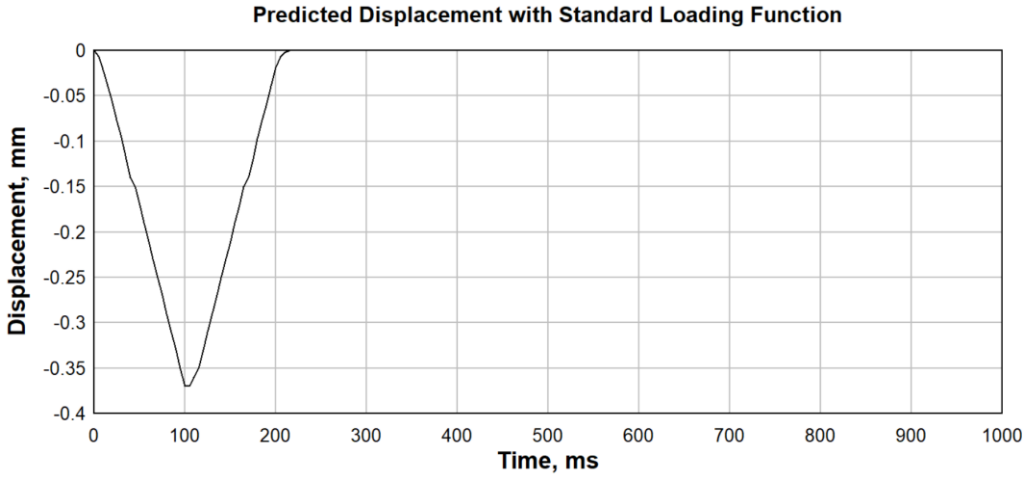


*Figure 54: Displacement with Standard Loading*

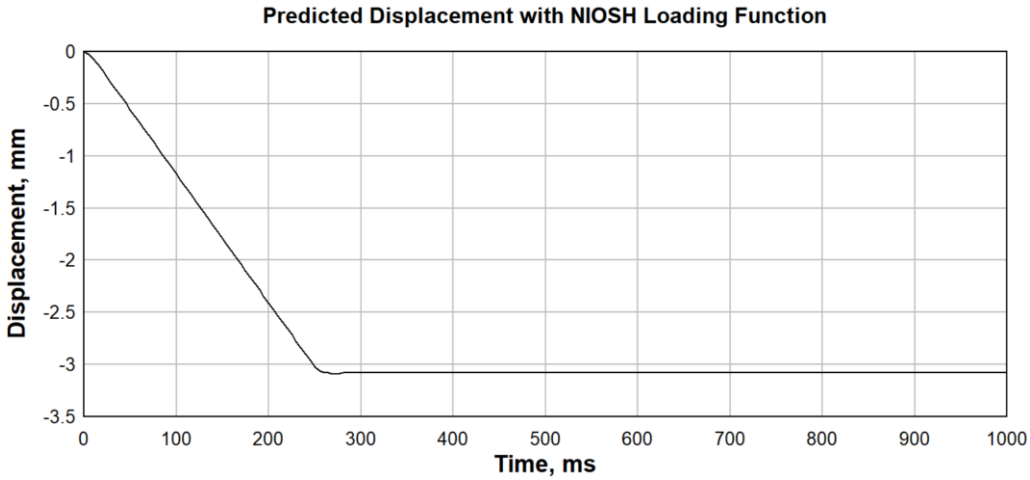


*Figure 55: Displacement with NIOSH Loading*

### *5.4.2 Study Two Results*

Increasing the Young's modulus did not dramatically change the profile shape of the displacement plots. However, the maximum displacement was smaller as shown in Figure 56.

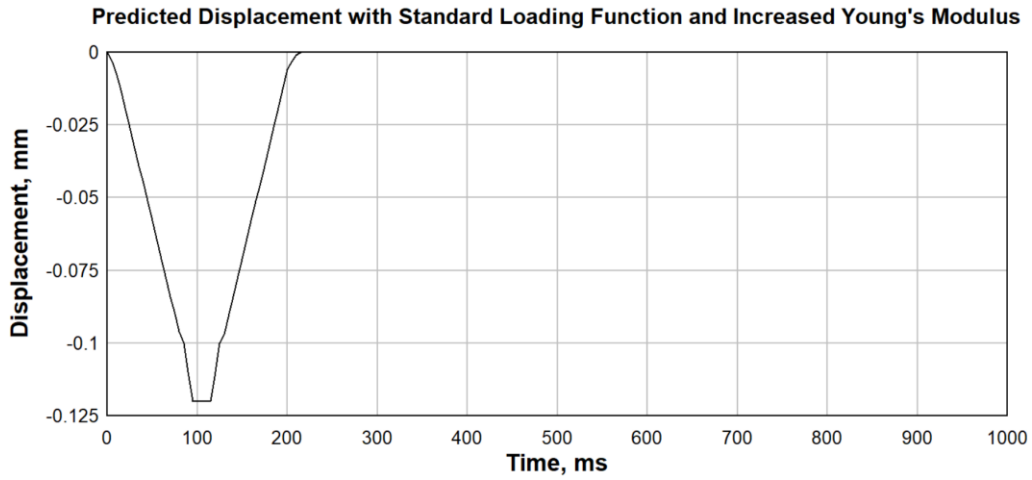


*Figure 56: Displacement with Increased Young's Modulus*

### *5.4.3 Stress Profile Along Boundary Results*

With the standard design curve loading function applied, stress values along the top and side of the wall were analyzed using MSC Marc. Starting at time zero, increments of 0.05 seconds were used to evaluate stress profile shapes, with the maximum stress being shown at approximately 0.30 seconds. Below, Figure 57 shows the stress profile of the boundary along the top of the wall and Figure 58 shows the stress profile of the boundary along the side of the wall for the same time increments.

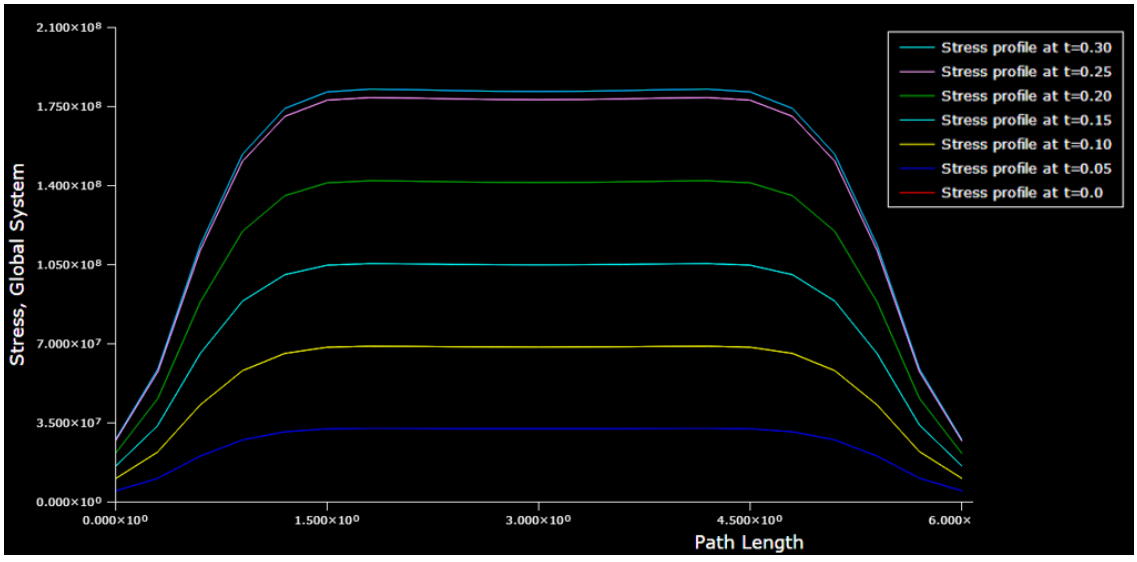


*Figure 57: Stress Profile Along Top of Wall*

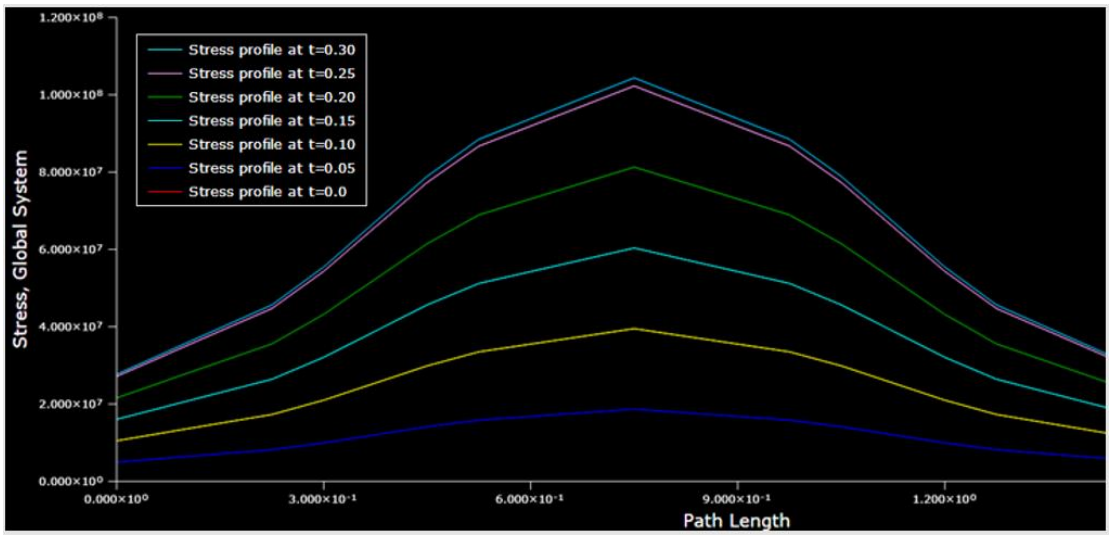


*Figure 58: Stress Profile along Side of Wall*

# 6 Chapter 6: DISCUSSION OF THE RESULTS

Chapter four included data collected during experimental testing, while chapter five provided results from modeling simulations. Here, Chapter six serves to connect and discuss findings from both.

## 6.1 Experimental Testing Results

The experimental testing described in this thesis can be divided into three categories. The first category was completed to determine the profile shape of high and low explosives. As expected, the high explosive charge created a pressure profile similar to an ideal pressure curve. The pressure profiles of methane explosions are not as widely studied as those for high explosives. It was expected that the methane would produce a profile with a lower peak pressure and longer duration. However, the specific wave shape was not known. Given the length of the scaled shocktube, and the relatively small volume of methane used, the explosion did not travel a distance great enough to transition from deflagration to detonation. When ignited, the methane produced pressures three times smaller than the high explosive, but with an extended duration produced an impulse almost twice as large as the high explosive. This relationship serves as the basis for understanding the differences in structural displacements examined in Chapter five and the second research question presented in Chapter one.

The second category of testing was completed to improve testing techniques for measuring pressures during a methane and coal dust explosion and to ultimately help answer the first research question presented. Very few testing facilities have ever created coal dust and methane explosions to record pressure readings. Throughout the course of this research, it was found that many of the devices used in previously conducted testing are now considered obsolete or are commercially unavailable. As no pressure recording devices have been in place during a mine disaster, the only source of knowledge used to create standards for mine seals and refuge chambers comes from laboratory testing. In this thesis, three different heat shielding mechanisms are examined and evaluated during both low and high heat conditions. Two of the three methods proved promising and are designed using the same principle. Both the UKERT and NIOSH devices work to limit heat exposure to the face of the pressure sensors. In testing, both methods produced similar pressure profiles. In contrast, the unprotected and 176M03 model sensors experienced thermal expansion and provided inaccurate readings.

The final category of experimental testing was completed using multiple electronic detonators, delayed to create an extended pressure event. Looking at readings collected by the sensor furthest from the detonators (Ch1), a single detonator produced a peak pressure of 18.1psi and an impulse of 35.3 psi-ms. When three charges are used at a 2ms delay, the peak pressure rises to 28.8 psi and an impulse value of 92.2. While three peaks are distinguishable in the 2ms pressure profile, it also produced the largest impulse value. When the delay between detonators is only 1ms, the peaks become less recognizable,

creating a more uniform wave shape. Dependent on what pressure and impulse is desired for specific testing, it is possible that multiple detonators could be used in conjunction to produce values similar to those experienced in a coal dust and methane explosion.

## 6.2 Finite Element Analysis Results

The last category of experimental research completed was designed to answer the third and final research question. However, additional structural analysis was needed to provide a compressive look at how structures behave in blast events. Figure 59 shows the progression of the structural analyses completed in Chapter five.

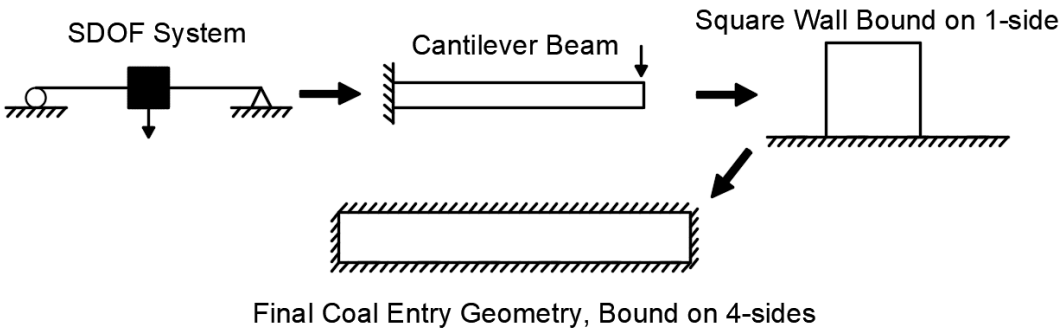


*Figure 59: Progression of Structural Analysis*

Because no specific design was being represented in the first three rounds of analysis, units of deformation are used as comparisons rather than physical data to be used in design work. The initial analysis was completed from individual calculations to account for particle displacement at increasing time intervals using differential equations. In the single degree of freedom analysis, a generic system was used to study the differences in displacement caused by two different loading profiles. The high explosive profile had a higher peak pressure value, shorter duration, and ultimately a smaller impulse value. The low explosive profile had a lower peak pressure value, longer duration, and ultimately a larger impulse value. As predicted, impulse is the driving factor in maximum displacement, not peak pressure. Another key point displayed in the dimensionless SDOF analysis, was the appearance of the sinusoidal motion in displacement over time. This oscillating pattern was found in all displacement profiles resulting from loading functions lasting less than 40 ms.

The four case studies completed with the cantilever beam each show an important concept of structural reaction to different pressure profiles. The first case studied the same concept as the SDOF software, using scaled high and low explosive profile loads. The beam analysis differs from the SDOF analysis as it was completed using Finite Element Analysis software. The resulting displacements from the FEA for case one did confirm that the higher impulse peak pressure curve would result in a larger displacement. Another way to

describe this phenomenon is in terms of energy. As impulse represents the energy of an explosion, the energy of a blast wave is directly related to the displacement experienced.

Case two of the beam analysis explored the relationship between loading profiles and displacement profiles. The effect of damping caused oscillations of displacement to cease after a period of time, at which point, the displacement profile was the same shape (a constant force) as the loading profile. While the varying low explosion profile caused a dynamic response that did not mirror the loading function. The distinction was made that when the quasi-static loading was released, the beam did respond dynamically and returned to its initial position.

Case three provides insight to how high explosive may be used to study realistic coal dust and methane explosions, which tend to produce pressure curves similar to low explosives. While the two loading profiles studied in case three vary dramatically in rise time, pressure duration, and overall wave shape, the resulting impulse values and displacements are almost identical. In comparison, case four ignores wave shape and focuses on the rise time of loading functions. As the rise time of the loading functions increase, the resulting displacements more closely resemble the shape of the loading function, with a dramatic change between 100 and 250 ms. Displacement amplitude increases with a smaller rise time while the period of the oscillations decreases. The results shown from these two case studies highlight the importance of consideration of both wave shape and rise time in structural displacement.

By varying damping constants, the beam example was used to calibrate a wall geometry to be used in the analysis. The wall geometry was further manipulated to reflect the width and height of a coal mine entry. The increase in bound wall perimeter, assigned a translational and rotational movement of zero, made the wall much less susceptible to movement. Further changes in boundary conditions, binding all four sides, resulted in little to no continued oscillations in further analyses. Additionally, it was shown that as the pressure duration increases, to values of 200 ms in the standard design curve and 1000 ms in the NIOSH recommended design curve, the wall no longer responds dynamically. Instead, displacement plots directly mirror loading plots. Because pressure application time plays such a crucial role in governing structural oscillation and displacements, design profiles and research conducted for the structural analysis should include a pressure duration. Infinite durations provide no practical direction to what seal designs should withstand.

Additionally, an infinite durational also means an infinite impulse is being applied to the structural. For these reasons, a maximum of 1000ms durations were used in this research. However, other sources do not describe the pressure duration in many recommend design profiles.

Though material properties for the wall do not accurately represent those found in actual mine seals, results showing stress values around the boundary of the wall provide locations where the highest stress values are recorded and where potential failures could occur. Overall, the highest stress values are found along the top off the wall, approximately 1.5 m in from each side. Similarly, the highest pressure felt along the side of the wall were also in the center, but the overall profile shape for stress along the vertical edge of the wall is much sharper than that for the top, with a smaller length experiencing peak stresses.

This thesis combines both experimental and theoretical work to answer three research questions. When studying dynamic and complex events such as mine explosions, it is important to find a balance between the two, to fully capitalize available technologies, while still approaching problems in a practical and realistic manner.

# 7 **Chapter 7:** CONCLUSIONS AND FUTURE WORK

Chapter seven serves as a conclusion to the work completed in this thesis. The initial three research questions are presented with conclusions. While the purpose of this research was to provide a better understanding of principles found in underground coal mine explosions, two specific novel contributions were made through the research completed.

It is known that the pressure and duration of a blast wave are directly related to the impulse, as impulse is equal to the integral of a pressure-time curve. What remains unclear is what pressure values and durations can be expected from a coal dust and methane explosion. Based on past research, both theoretical and experimental, along with the reverse engineering of mine disasters, a wide variety of pressure values could be expected from coal dust and methane explosions. Pressures ranging from 4-120 psi have been estimated. Due to the interference of heat, pressure readings taken during coal dust and methane explosions for this research were limited. Given the results of shielding mechanism testing, both the NIOSH and UKERT shielding techniques were recommended for collecting pressure data in the high temperature conditions of a coal dust and methane explosion. While it was determined that none of the shielding mechanism significantly reduce pressure values, only the UKERT and NIOSH designs were considered adequate at negating heat interference in pressure readings.

As shown in multiple tests, a higher impulse value (higher energy value) can often lead to a higher predicted displacement. While not the only contributing factor to displacement, impulse should be taken into consideration when making design recommendations for underground mine structures. As shown in multiple testing, the rise time of a pressure function also plays an important role in determining displacement. Ultimately the combination of these two characteristics: impulse and rise time, play a much more influential role in determining structural response than a singular peak pressure value.

The construction of a testing facility to conduct full scale coal dust and methane testing is rare, time consuming, and expensive. For these reasons, it is often not practical for feasible for many research groups to conduct full scale coal dust and methane explosion testing. Industry standards include using 20-L chambers for testing, but results from these scaled test do not always translate properly for full scale events. Initial testing using multiple high explosive charges in this research proved promising, with larger impulse values created and overall wave shapes altered. Further work can be completed to refine the delay sequence to alter pressure waves more precisely.

While the main purpose of the SDOF and FEA was to study the influence of impulse on structural displacement, additional trends became apparent throughout the process of completing the structural analysis portion of this research, they include:

- The smaller the rise time of the loading function, the smaller the period of the oscillation for the resulting displacement function.
- Increasing Young's modulus of a structure will decrease displacement
- When bound on all four sides, models in MSC-Marc would stop oscillations after ½ of the period.
- The timing of peak displacements dose not always correspond to the timing of peak pressures.
- Increasing the duration of a loading function will eventually cause the displacement function to mirror the shape of the loading function.
- The highest stress values along the boundary of a mine seal can be found along the inner length of the longest sides and extends over the majority of that length.

While many important distinctions are shown in this thesis, as described above, two main novel contributions can be given:

- The representation of influence that impulse, rise time, and overall wave shape has on structural displacement
- Design and testing of shielding techniques to collect pressure data in high temperature environments

## 7.1 Future Work

While each of the research questions have been addressed through this thesis, there are improvements that can be made for future research. This includes:

1. Extending the FEA to include geometries and material properties to more accurately represent mine seals to provide a more compressive study of structural responses during a mine explosion.

2. Completing FEA where structures move into the plastic-elastic and ultimately plastic regions of the stress strain curve to allow for permanent failures to occur.

3. Conducting test in UKERT's full scale shock tube once it is completed. This structure is currently being built by the UKERT team and is scheduled to be completed by early 2019. This will allow for more representative methane and coal dust explosion conditions to be created for testing. Purposed testing for the new shocktube includes

    a. Testing of heat shielding devices in open areas;
    b. Testing of physical structures under high and low explosive conditions and recording strain values experienced;

c. And, testing of temperatures and peak pressures experienced during methane and coal dust explosion.

# Appendix I

*Methane and Coal Dust, Test 1 and 2 data for Shielding techniques*

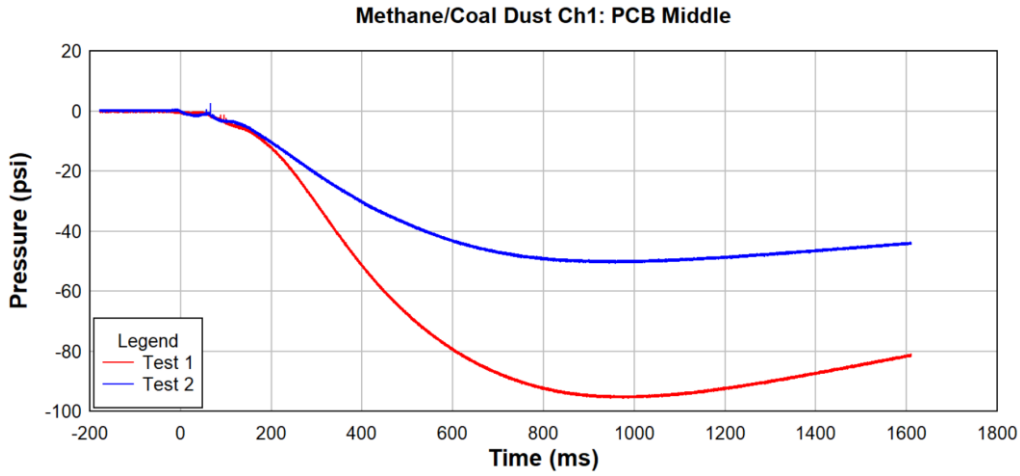


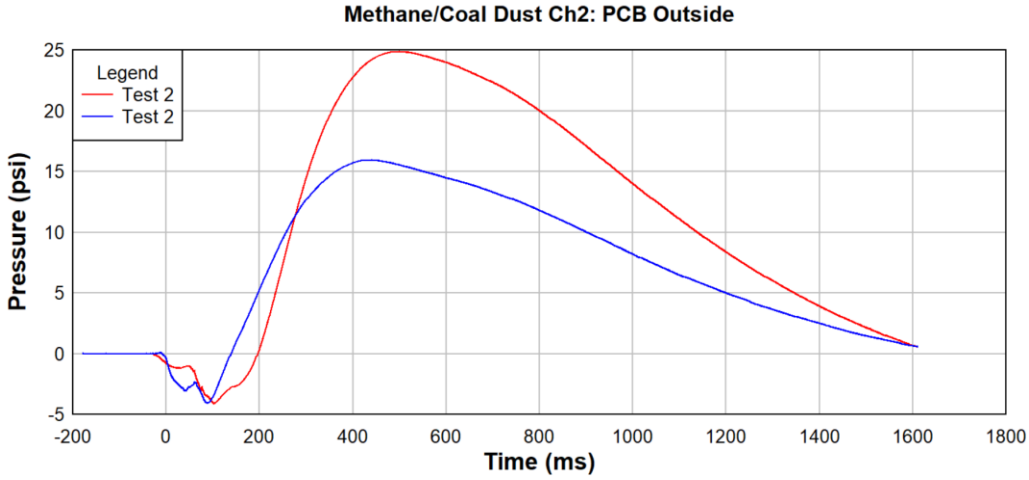


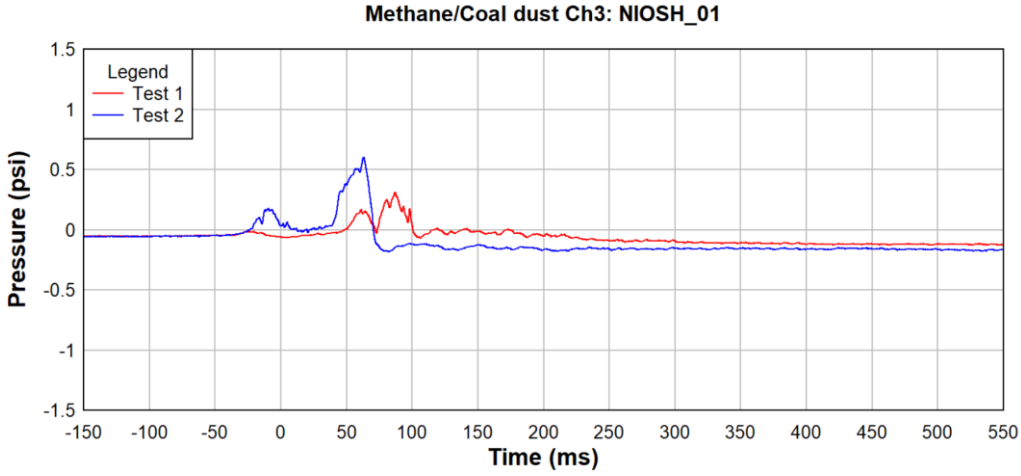

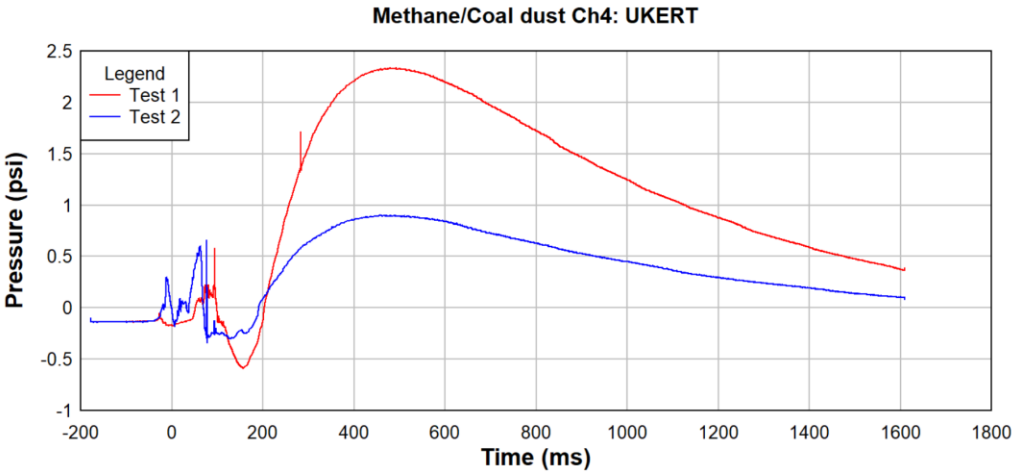
Methane/Coal dust Ch4: UKERT
Legend
Test 1
Test 2
Pressure (psi)
Time (ms)

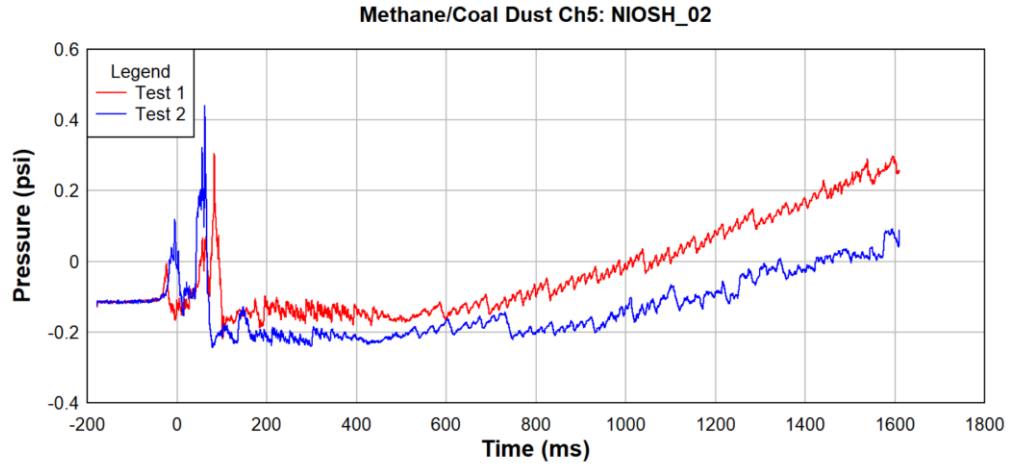
Methane/Coal Dust Ch5: NIOSH_02
Legend
Test 1
Test 2
Pressure (psi)
Time (ms)

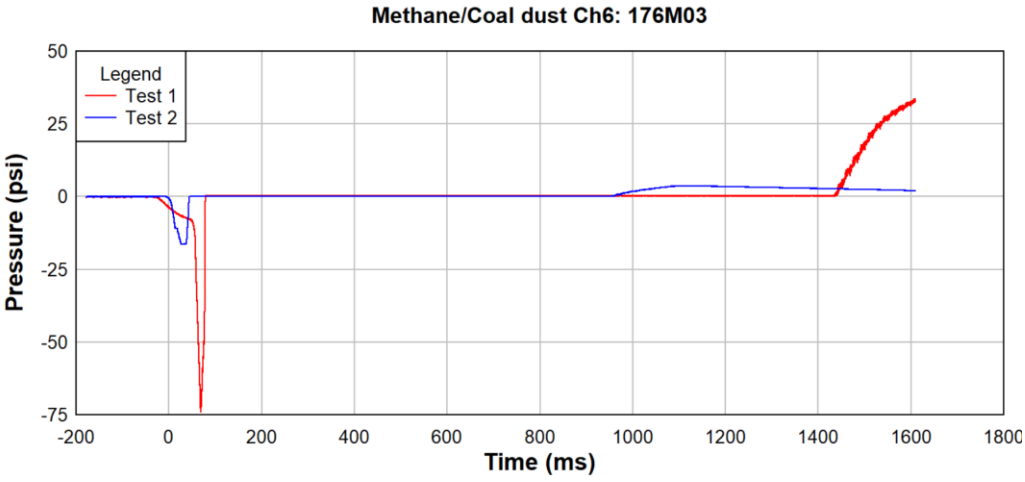
Methane/Coal dust Ch6: 176M03
Legend
Test 1
Test 2
Pressure (psi)
Time (ms)

*Images from MSC Marc FEA Software*

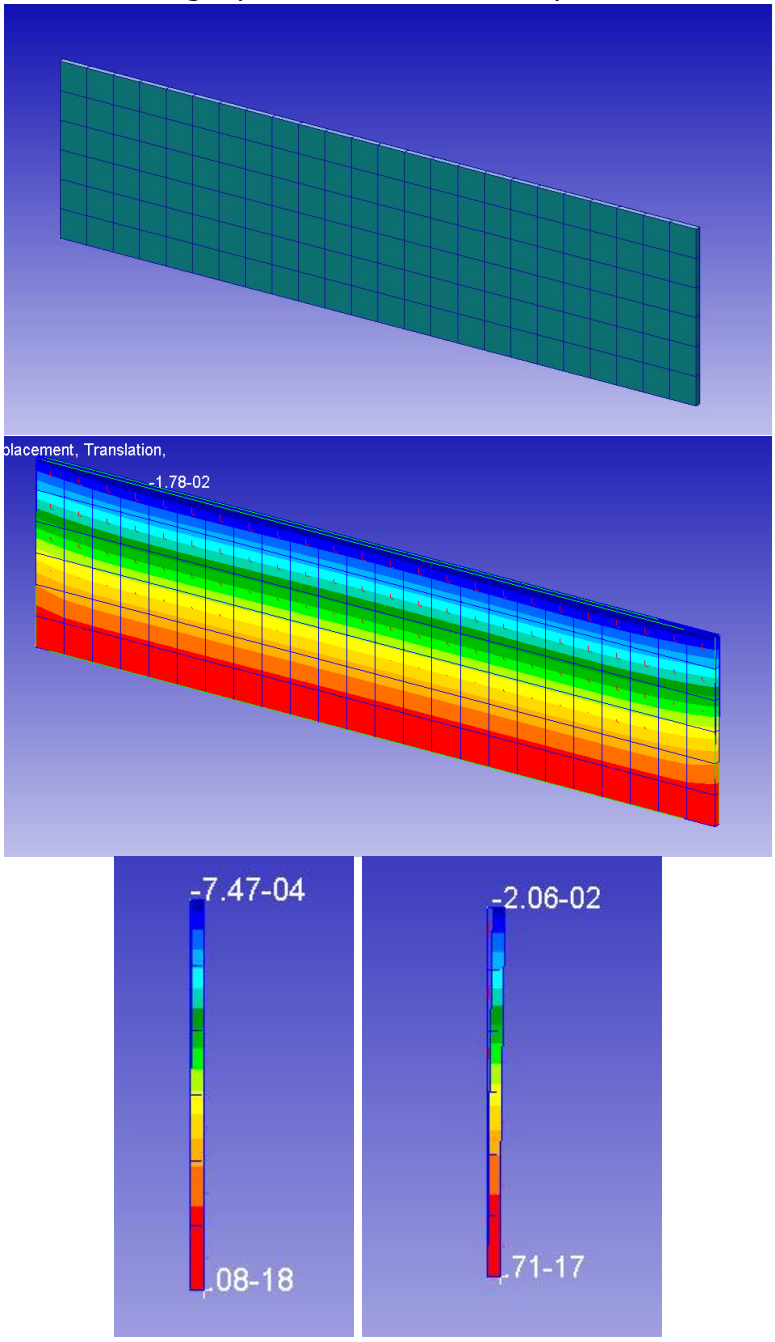

# References


Agrawal, V., & Bhattacharya, K. (2014). Shock wave propagation through a model one dimensional heterogeneous medium. *International Journal of Solids and Structures*, *51*(21-22), 3604-3618.

Ajrash, M. J., Zanganeh, J., & Moghtaderi, B. (2016). Effects of ignition energy on fire and explosion characteristics of dilute hybrid fuel in ventilation air methane. *Journal of Loss Prevention in the Process Industries*, *40*, 207-216.

Alonso, F. D., Ferradás, E. G., Pérez, J. F. S., Aznar, A. M., Gimeno, J. R., & Alonso, J. M. (2006). Characteristic overpressure–impulse–distance curves for the detonation of explosives, pyrotechnics or unstable substances. *Journal of Loss Prevention in the Process Industries*, *19*(6), 724-728.

Baker, W. E. (1973). *Explosions in air*. University of Texas press.

Biggs, J. M., (1964). *Introduction to structural dynamics* (Vol. 3). New York: McGraw-Hill.

Cashdollar, K. L. (1996). Coal dust explosibility. *Journal of Loss Prevention in the Process Industries*, *9*(1), 65-76.

Cashdollar, K. L., & Hertzberg, M. (1985). 20-l explosibility test chamber for dusts and gases. *Review of Scientific Instruments*, *56*(4), 596-602.

Chawla, N., Amyotte, P. R., & Pegg, M. J. (1996). A comparison of experimental methods to determine the minimum explosible concentration of dusts. *Fuel*, *75*(6), 654-658.

du Plessis, J. J. L., Saleh, J. K., & Phillips, H. R. (2017) Coal Mine Explosions and the Development of Mitigating Controls, 16th US Mine Ventilation Conference, Colorado School of Mines, 2017

Eades, R. (2016). Modern Rock Dust Development and Evaluation for Use in Underground Coal Mines (Master's thesis) Retrieved from https://uknowledge.uky.edu/cgi/viewcontent.cgi?article= 1030&context=mng_etds

Eades, R., Perry, K., Johnson, C., & Miller, J. (2018). Evaluation of the 20 L dust explosibility testing chamber and comparison to a modified 38 L vessel for underground coal. *International Journal of Mining Science and Technology.*

EIA, U. Annual Coal Report 2016 (2017). *Tables*.

Glasstone, S., & Dolan, P. J. (1977). *The effects of nuclear weapons*. Department of Defense Washington DC.

Hedrick, K., Nicola, G. (2011) Invesitgative Report Portal Methane and Multi-Gas Detectors Recovered from a Mine Explosion at Performance Coal Company Upper Big Branch Mine-South Montcoal (Raleigh County), WV. MSHA

Humphreys, D., Collecutt, G., & Proud, D. (2010). CFD simulation of underground coal dust explosions and active explosion barriers. In Proceedings of the 10th Underground Coal Operators' Conference, University of Wollongong & the Australasian Institute of Mining and Metallurgy, pp. 330–338 .

Karlos, V., & Solomos, G. (2013). Calculation of blast loads for application to structural components. *Luxembourg: Publications Office of the European Union*.

Kuchta. J. M, (1985) investigation of fire and explosion accidents in the chemical. mining, and fuel-related industries - a manual (84 pp.). US Bureau of Mines Bulletin 680.

Meyr Jr, R. A. (2013). Development of 15 psi safe haven polycarbonate walls for use in underground coal mines. (Master's thesis) Retrieved from: https://uknowledge.uky.edu/cgi/viewcontent.cgi?referer=https://www.google.com/&httpsredir=1&article=1002&context=mng_etds

Nagy, J. (1981). The explosion hazard in mining. In U.S. Mine Safety and Health Administration, IR 1119 (69 pp).

Ngo, T., Mendis, P., Gupta, A., & Ramsay, J. (2007). Blast loading and blast effects on structures–an overview. *Electronic Journal of Structural Engineering*, 7(S1), 76-91.

QinetiQ North America & Foster-Miller Inc. (2008). System Reliability and Environmental Survivability-Vol 1 (Report No. 1) NIOSH

Sapko, M. J., Harteis, S. P., & Weiss, E. S. (2008). Comparison of methods: dynamic versus hydrostatic testing of mine ventilation seals. *Mining Engineering*, 60(9), 143.

Sapko, M. J., Weiss, E. S., Cashdollar, K. L., & Zlochower, I. A. (2000). Experimental mine and laboratory dust explosion research at NIOSH. *Journal of Loss Prevention in the Process Industries*, *13*(3-5), 229-242.

Wu, H. W., Gillies, A. D. S., Oberholzer, J. W., & Davis, R. (2009). Australian Sealing Practice and use of Risk Assessment Criteria - ACARP Project C17015. In Proceedings of the Queensland Mining Industry Health and Safety Conference, Townsville, Queensland, Australia, August 23–26.

Zipf Jr, R. K., Brune, J. F., & Thimons, E. D. (2009) Explosion pressure design criteria for seals in us coal mines–an update on work at NIOSH, Ninth International Mine Ventilation Congress, Delhi, India, 2009

# VITA

Brooklynn Hope Yonts

## Education

Master of Science in Mining Engineering at University of Kentucky, August 2017-present. Thesis title: “Analysis of Underground Coal Mine Structures Subjected to Dynamic Events.”

Bachelor of Science (May 2017) in Mining Engineering, University of Kentucky, Lexington, Kentucky.

## Academic Employment

Graduate Teaching Assistant, Department of Mining Engineering, University of Kentucky, MNG201 August 2018- present.

Research Assistant to Dr. Jhon Silva, Department of Mining Engineering, University of Kentucky, May 2017-present.

## Scholastic and Professional Honors

Outstanding Senior for UK College of Engineering 2017

Watchman Award 2017

Academic Excellence Award 2017

Margaret Ingles SWE Graduate Fellowship 2017